Title

PD-L1/L2 protein levels rapidly increase on monocytes via trogocytosis from tumor cells in classical Hodgkin lymphoma

Authors

Masaharu Kawashima[1, 2], Joaquim Carreras[3], Hiroshi Higuchi[1, 4], Ryutaro Kotaki[1], Takahiro Hoshina[1, 5], Kazuki Okuyama[1], Naoto Suzuki[1, 6, 7], Masatoshi Kakizaki[1], Yuji Miyatake[1], Kiyoshi Ando[8], Masafumi Nakayama[9], Shinjiro Umezu[10], Ryouichi Horie[11], Yuriko Higuchi[12], Koko Katagiri[6], Susumu Goyama[5], Toshio Kitamura[5], Kenji Chamoto[13], Shingo Yano[2], Naoya Nakamura[3], and Ai Kotani[1, 14, 15]

Department:

[1]Department of Hematological Malignancy, Institute of Medical Science, Tokai University, Isehara, Kanagawa, Japan.

[2]Division of Clinical Oncology and Hematology, Jikei University School of Medicine, Minato-ku, Tokyo, Japan.

[3]Department of Pathology, Tokai University School of Medicine, Isehara, Kanagawa, Japan.

[4]Research Institute of Science and Technology, Tokai University, Hiratsuka, Kanagawa, Japan.

[5]Division of Cellular Therapy, Advanced Clinical Research Center, The Institute of Medical Science, The University of Tokyo, Minato-ku, Tokyo, Japan.

[6]Department of Biosciences, School of Science, Kitasato University, Sagamihara, Kanagawa, Japan.

[7]Department of Computational Biology and Medical Sciences, Graduate School of Frontier Sciences, The University of Tokyo, Kashiwa, Chiba, Japan.

[8]Department of Hematology and Oncology, Tokai University School of Medicine, Isehara, Kanagawa, Japan.

[9]Frontier Research Institute for Interdisciplinary Sciences, Tohoku University, Aoba-ku, Sendai, Japan.

[10]Department of Modern Mechanical Engineering Waseda University, Shinjuku-ku, Tokyo, Japan.

[11]Division of Hematology, Department of Laboratory Sciences, School of Allied Health Sciences, Kitasato University, Sagamihara, Kanagawa, Japan.

[12]Department of Drug Delivery Research, Graduate School of Pharmaceutical Sciences, Kyoto University, Sakyo-ku, Kyoto, Japan.

[13]Department of Immunology and Genomic Medicine, Graduate School of Medicine, Kyoto University, Kyoto, Japan.

[14]Precursory Research for Embryonic Science and Technology, Japan Science and Technology Agency, Saitama, Japan.

[15]AMED-PRIME, Japan Agency for Medical Research and Development, Tokyo, Japan.

Correspondence author:

Ai Kotani, MD PhD

Department of Hematological Malignancy, Institute of Medical Science, Tokai University, Isehara, Kanagawa, Japan.

Email: aikotani@k-lab.jp

Abstract

In classical Hodgkin lymphoma (cHL)—characterized by the presence of Hodgkin and Reed-Sternberg (HRS) cells—tumor-associated macrophages (TAMs) play a pivotal role in tumor formation. However, the significance of direct contact between HRS cells and TAMs has not been elucidated. HRS cells and TAMs are known to express PD-L1, which leads to PD-1^+ $CD4^+$ T cell exhaustion in cHL. Here, we found that PD-L1/L2 expression was elevated in monocytes co-cultured with HRS cells within one hour, but not in monocytes cultured with supernatants of HRS cells. Immunofluorescence analysis of PD-L1/L2 revealed that their upregulation resulted in membrane transfer called “trogocytosis” from HRS cells to monocytes. PD-L1/L2 upregulation was not observed in monocytes co-cultured with PD-L1/L2-deficient HRS cells, validating the hypothesis that there is a direct transfer of PD-L1/L2 from HRS cells to monocytes. In the patients, both ligands (PD-L1/L2) were upregulated in TAMs in contact with HRS cells, but not in TAMs distant from HRS cells, suggesting that trogocytosis occurs in cHL patients. Taken together, trogocytosis may be one of the mechanisms that induces rapid upregulation of PD-L1/L2 in monocytes to evade antitumor immunity through the suppression of T cells as mediated by MHC antigen presentation.

Introduction

Classical Hodgkin lymphoma (cHL) is a unique subtype of lymphoma characterized by a small population of the tumor cells known as Hodgkin and Reed-Sternberg (HRS) cells[1-4]. The tumor immune microenvironment (TIME), which consists of various immune cells, such as B cells, T cells, and macrophages, has been reported to play a crucial role in cHL[1]. Infiltration of tumor-associated macrophages (TAMs) has been correlated with poor prognosis of cHL, suggesting that TAMs play a key role in the TIME[5-7]. An increased number of peripheral blood monocytes in cHL patients has also been associated with poor prognosis[8, 9]. Thus, regulation of TAMs and monocytes have been proposed as potential mechanisms for treatment of cHL.

Several humoral factors that regulate TAMs, specifically, cytokines and chemokines, such as the macrophage migration inhibitory factor, CX3CR1, and the colony stimulating factor 1 receptor (CSF1R), are involved in the development of cHL[10, 11]. CSF1R, which is essential for the differentiation of macrophages[12, 13], has been extensively studied through the use of inhibitors. However, inhibition of CSF1R led to limited tumor suppression in cHL[13], suggesting that other mechanisms and humoral factors are involved in the formation and regulation of TAMs. While several studies have revealed that TAMs colocalize with HRS cells in a microenvironmental niche[2, 3, 14], the role of TAMs in the formation of TIME and in the progression of cHL remains elusive.

Most HRS cells have copy number alterations on 9p24.1, leading to the overexpression of the programmed cell death 1 (PD-1) ligands, PD-L1 and PD-L2, in tumor cells[15-17]. Once PD-L1/L2 binds with PD-1 on the T cell surface, the T cell immune response is negatively regulated. The critical role of the PD-1/PD-L axis in cHL development is supported by the efficacy of anti-PD-1 antibody treatment[18-22]. PD-L1 and PD-L2 expression in antigen-presenting cells (APCs), including monocytes and macrophages, are linked to tumor progression[23-26]. Upregulation of PD-L1 in TAMs occurs in cHL[27], and the proportion of PD-L1$^+$ monocytes was higher in the peripheral blood of cHL patients than in the peripheral blood of either diffuse large B cell lymphoma patients or healthy donors[28]. These studies suggest that PD-L1 expression in TAMs and monocytes is important in the development of cHL.

Here, we studied the effect of direct contact between HRS cells and monocytes on PD-L1/L2 expression. We found that membrane transfer from HRS cells to monocytes, known as “trogocytosis”[29-31], was induced by direct contact. In general, trogocytosis whose rate is affected in a cell-cell contact-dependent manner, is a rapid process, which can be distinguished from other intercellular transfer mechanisms, such as exocytosis[31]. Trogocytosis mediated the transfer of PD-L1/L2 from HRS cells to monocytes within an hour, which was validated using PD-L1/L2-deficient HRS cells. Importantly, immunostaining of patient tissue specimens demonstrated that the expression of PD-L1/L2 was higher in

103 macrophages in contact with HRS cells compared to those that were not in contact with HRS

104 cells, suggesting that trogocytosis occurs in cHL patients.

105

Methods

Cells

L-591, L-1236, and L-428 cell lines are derived from cHL patients. THP-1 cells are derived from patients with acute monocytic leukemia. These cell lines were obtained from DSMZ (Braunschweig, Germany).

Trogocytosis observation by confocal microscopy

HRS cells were labeled with PKH26 (SIGMA-ALDRICH) or stained as follows: APC-conjugated anti-human PD-L1 (29E.2A3, BioLegend) and PE-conjugated anti-human PD-L2 (24F.10C12, BioLegend) or APC-conjugated anti-human CD30 (BY88, BioLegend). The membrane of monocytes was labeled with PKH67 and the nuclei were labeled with Hoechst 33258. Then, 1×10^5 HRS cells and 1×10^5 monocytes were placed in a 96-well (200 μl/well) plate. Cells were observed via confocal microscopy after one hour of incubation at 37℃.

Immunohistochemistry and digital image quantification of PD-L1/L2 in TAMs in cHL

To evaluate the differential expression of PD-L1/L2 on macrophages in contact with the HRS cells, as compared to the distant ones in cHL, PD-L1/L2 immunohistochemical (IHC) staining was performed on 38 cases using paraffin-embedded whole-tissue sections at

Tokai University (Pathology Department), using single and double staining procedures with CD163. The study was approved by the Institutional Review Board (IRB18R-143) of Tokai University. Informed consent was provided according to the Helsinki Declaration. The summary of IHC details are shown in Supplemental Methods.

Statistical analysis

Statistical significance was assessed by Student's t-test, Wilcoxon signed-rank test or Friedman's test. Bonferroni correction was used for multiple comparisons. A *P*-value < 0.05 was considered statistically significant.

Results

Direct contact was maintained between monocytes and HRS cell lines

To assess direct contact between monocytes and HRS cell lines, THP-1 cells derived from human monocytic leukemia cells, or primary monocytes isolated from healthy donors, were co-cultured with HRS cell lines (L-591, L-1236) in semi-solid culture. The time-lapse analysis revealed that both THP-1 cells and monocytes were motile and maintained direct contact with the HRS cell lines. (Figure 1A, and Supplemental Video 1, 2).

Additionally, the transwell assay indicated that the migration of L-1236 toward the monocytes was slightly observed (Figure 1B). In contrast, both supernatants of L-591 and L-1236 cells induced significant migration of monocytes (Figure 1C). These results suggest that monocytes migrated to HRS cells, leading to sustained direct contact between these two cell types.

PD-L1/L2 expression was upregulated in monocytes by direct contact with HRS cells

In order to explore the biological significance of direct contact between HRS cells and monocytes, we investigated the expression levels of PD-L1/L2 in co-cultures of HRS cells and monocytes. PD-L1 expression on THP-1 cells was upregulated after THP-1 co-culture with L-1236; however, PD-L1 expression was not affected by the supernatant from the L-1236 cell culture (Supplemental Figure 1). Notably, both PD-L1 and PD-L2 were

upregulated in the primary monocytes only one hour after co-culture with L-1236 cells, while PD-L1/L2 expression remained unaffected by the L-1236 culture supernatant. PD-L1 was also slightly upregulated by co-culture with L-591 cells. In contrast, no PD-L1/L2 upregulation was observed in the co-culture with L-428 cells (Figure 2A-2C).

To investigate the effects of the humoral factors secreted by HRS cells on the expression of PD-L1/L2 in monocytes, human peripheral blood mononuclear cells (PBMCs) were treated with culture supernatants of HRS cells for 24 hours. The culture supernatant of L-591 cells upregulated both PD-L1 and PD-L2 in monocytes, while the supernatant of L-1236 cells elevated PD-L1 but not PD-L2 expression. In contrast, the supernatant of L-428 cells did not affect PD-L1 and PD-L2 expression (Supplemental Figure 2).

These results demonstrated that both the humoral factors secreted by the HRS cells and direct contact between HRS cells and monocytes elevate PD-L1/L2 expression in monocytes under 24 hours co-culture. Notably, supernatants of HRS cells that contained cytokines and exosomes secreted from HRS cells did not increase PD-L1/L2 expression in monocytes after one hour of culture. Furthermore, we analyzed whether exosomes from HRS cell lines got incorporated into the monocytes after one hour or 24 hours of treatment with purified exosomes (Supplemental Figure 3A, 3B). While the exosomes got incorporated in over 60% of the monocytes incorporated exosomes after 24 hours treatment, 10% or fewer monocytes exhibited exosome incorporation after one hour of treatment. Even the

monocytes incorporating the $PKH^{+}PI^{-}$ exosomes did not exhibit any upregulation of PD-L1/L2 (Supplemental Figure 3C). These results indicate that exosomes secreted by HRS cells do not lead to the upregulation of PD-L1/L2 in a short time. However, even brief direct contact with HRS for five minutes induced PD-L1/L2 upregulation upon using PD-L1/L2 overexpressing L-428 ($L\text{-}428^{L1++OE}$). (Figure 2D).

PD-L1/L2 were transferred from HRS cells to monocytes

We further investigated the mechanism of PD-L1/L2 upregulation in monocytes by studying the effects of short-term direct contact with HRS cells. Due to the rapid upregulation of PD-L1/L2, we focused on trogocytosis from HRS cells to monocytes. Trogocytosis is defined as the bidirectional movement of molecules between interacting cells or towards cells to which a donor cell is connected via the interchange of plasma membrane fragments[29-31], and trogocytosis occurred even within minutes[32]. The results of confocal microscopy revealed trogocytosis-mediated transfer of a fluorescent dye (PKH26) between HRS cells and monocytes (Figure 3A, Supplemental Figure 4), suggesting that trogocytosis is potentially involved in the upregulation of PD-L1/L2 on monocytes. Next, we labeled PD-L1/L2 on the HRS cell surface with fluorescence dye-conjugated antibodies, and the cells were co-cultured with PKH67-labeled monocytes. Confocal microscopy showed colocalization of

PD-L1 and PD-L2 with PKH67, indicating the direct transfer of these molecules between HRS cells and monocytes (Figure 3B and 3C).

Since trogocytosis is a phenomenon in which all membrane fragments of donor cells are transferred to recipient cells, including the immune synapse[33, 34], the level of protein expression in the donor cells is believed to affect the amount of transferred protein. Flow cytometry analysis showed that L-1236 cells had higher expression levels of PD-L1 and PD-L2 than L-591 and L-428 cells (Figure 3D), which was consistent with the observed increase of PD-L1/L2 in monocytes when HRS cell lines were added to the culture (Figure 2B, 2C). The amount of PD-L1/L2 appeared to be unchanged in L-1236 after co-culture with monocytes despite the transfer (Supplemental Figure 5); this might be due to high basal levels of PD-L1/L2 expression in L-1236 cells. Moreover, CD30, which is strongly expressed in HRS cells, was also transferred from HRS cells to monocytes (Figure 3D, 3E). Again, the amount of CD30 in the monocytes correlated with the expression levels of CD30 in HRS cell lines (Figure 3F).

Co-culture with PD-L1/L2-deficient HRS cells did not affect PD-L1/L2 expression in monocytes

Considering trogocytosis-mediated rapid protein transfer, we hypothesized that the PD-L1/L2 expression levels of the HRS cell surfaces would determine the rate of increase of

monocytes in direct contact with both cells. Indeed, PD-L1/L2 expression remained unchanged in monocytes co-cultured with PD-L1/L2-deficient L-1236 cells and control cells (L-1236$^{L1/L2KO}$ and L-1236^{Vector} in Figure 4A) established by CRISPR/Cas9-mediated genome editing (Figure 4B). Conversely, CD30 was equally upregulated in monocytes co-cultured with L-1236$^{L1/L2KO}$ and L-1236^{Vector} (Figure 4B). Taken together, these results suggest that rapid upregulation of PD-L1/L2 in monocytes was induced by trogocytosis.

Furthermore, PD-L1/L2 expression on the monocytes co-cultured with PD-L1/L2 overexpressing L-428 cells (L-428$^{L1/L2++OE}$ in Figure 4C) was considerably upregulated, as compared with that of the control L-428 cells (L-428^{Vector}) (Figure 4D). Indeed, between the two PD-L1/L2 overexpressing L-428 cell lines, which showed different expression levels of PD-L1/L2 (L-428$^{L1/L2++OE}$ and L-428 $^{L1/L2+OE}$ in Supplemental Figure 6A), L-428$^{L1/L2++OE}$ cells with higher expression of PD-L1/L2 upregulated PD-L1/L2 in monocytes more substantially than L-428$^{L1/L2+OE}$ with lower expression of PD-L1/L2 did (Supplemental Figure 6B). The upregulation correlated with PD-L1/L2 expression levels in HRS cells, suggesting trogocytosis-mediated upregulation.

PD-L1 on THP-1 cells acquired from HRS cells has an inhibitory effect on CD3$^+$ T cells

Next, we explored the T cell inhibitory effect of PD-L1 on monocytes acquired by HRS cells using THP-1, human monocytic leukemia cells. We found that PD-L1 on isolated THP-1 cells

acquired from HRS cells did not sustain expression long term, and most of the transferred PD-L1 had diminished by 6 hours post-isolation (Supplemental Figure 7). Thus, we tried to determine the T cell inhibitory effect of isolated THP-1 cells that have acquired PD-L1 from HRS cells in an early time course of after isolation.

Expression of CD69, IL-2, and IFN-γ in the $CD3^+$ T cells isolated after the coculture with THP-1 cells where trogocytosis was caused by L-428^{Vector} cells (trog L-428^{Vector}), or those where by L-428^{L1++OE} cells (trogL-428^{L1++OE}), was evaluated. qPCR analysis for cells co-cultured with $CD3^+$ + isolated each THP-1 cells revealed that expression of CD69, IL-2, and IFN-γ mRNA of $CD3^+$ + THP-1 (trogL-428^{L1++OE}) was lower than that of $CD3^+$ + THP-1 (trogL-428^{Vector}) (Figure 5A). Further, secretion of IFN-γ of $CD3^+$ + THP-1 (trogL-428^{L1++OE}) was reduced compared to that of $CD3^+$ + THP-1 (trogL-428^{Vector}) (Figure 5B). These data indicated that THP-1 cells acquired PD-L1 from HRS cells have an inhibitory effect on $CD3^+$ T cells.

Expression of PD-L1/L2 was higher in TAMs in direct contact with HRS cells than in TAMs distant from HRS cells

Finally, we investigated the expression of PD-L1/L2 *in vivo* using human tissue samples. Characteristics of patients in the current study are shown in Supplemental Table 1. Topological analysis for PD-L1/L2 expression on TAMs was performed to verify trogocytosis

248 in patient tissue samples. The evaluation fields were separated into HRS^+ and HRS^- areas,
249 and the TAMs were further classified as follows: (1) “HRS-contacted” and (2) “HRS-close” in
250 the HRS^+ area; and (3) “HRS-distant” in the HRS^- area as described in Figure 6A and
251 Supplemental Figure 8. Both PD-L1 and PD-L2 expression were significantly elevated in
252 HRS-contacted TAMs compared to HRS-close and HRS-distant TAMs (Figure 6B) based on
253 the pathologist’s quantification. In contrast, PD-L2 expression was not significantly different
254 between HRS-close and HRS-distant TAMs, while PD-L1 expression was higher in
255 HRS-close TAMs than in HRS-distant ones. Taken together, these results suggest that
256 proximity to HRS cells more significantly affects PD-L1 than PD-L2 expressions in TAMs.
257 Details are listed in Supplemental Table 2 and Supplemental Figure 9.

258 To validate the results, Image J was used for digital image quantification. PD-L1/L2
259 expression in TAMs near the HRS cells were higher compared to HRS-distant ones as
260 evaluated by pathologists (Supplemental Table 3 and Supplemental Figure 10). The
261 analysis was repeated to stratify the results based on histological subtype (mixed cellularity
262 or nodular sclerosis), Epstein-Barr virus (positive or negative), and age (< 50 or ≥ 50), and
263 no significant differences were found (Supplemental Figure 11-16). However, we cannot
264 draw definite conclusions because of the small sample size.

265 We also noted that in more than half the cases, HRS-contacted TAMs also had
266 expression of CD30. Since CD30 is highly expressed in HRS cells, this observation

suggests that transfer of CD30 also occurs from HRS cells to TAMs (Figure 6C and Supplemental Table 4). Collectively, these results support our *in vitro* observations that trogocytosis is at least partly involved in the upregulation of PD-L1/L2 in TAMs in cHL patients.

Discussion

In the current study, we found that the expression of PD-L1/L2 in monocytes increased by trogocytosis from HRS cells to monocytes (Figure 2, 3). Indeed, analysis of human tissue specimens revealed that the expression of PD-L1/L2 in TAMs that were in contact with HRS cells was highest in the TAMs that infiltrated the tumor tissue. This suggests that PD-L1/L2 transfer from HRS cells to TAMs occurs in cHL patients (Figure 6). Based on the results, we concluded that PD-L1/L2 on the surface of peripheral blood monocytes recruited to the tumor tissue are promptly upregulated by direct contact with HRS cells. This may, in turn, play an important role in tumor progression in cHL through T cell suppression via the PD-1 and PD-L1/L2 axis (Figure 7).

Anti-PD-1 treatment in cHL has a good overall response rate in the range of 65%-87%[18-22]. Mediation of the PD-1 and PD-L1/L2 axis by major histocompatibility complex (MHC) class II antigen presentation is crucial for tumor formation[35-37]. HRS cells frequently have defects in MHC class I expression[38, 39]. Therefore, the expression of PD-L1/L2 in monocytes and antigen-presenting cells (APCs), which both express MHC class II, in the cHL TIME may explain the efficacy of anti-PD-1 treatment in cHL. Because $CD8^+$ cytotoxic T cells recognize tumor antigens presented by MHC class I molecules[40, 41], $CD8^+$ effector T cells are not entirely responsible for the dramatic efficacy of anti-PD-1 treatment. In contrast, the effector $CD4^+$ T cells exert critical immunosuppressive functions and have more critical

roles in cHL progression[42, 43]. Indeed, high numbers of PD-1$^+$ CD4$^+$ T cells are abundant in surrounding HRS cells[14]. Additionally, mass cytometry fractions have shown that the tumor tissue in cHL mainly consisted of exhausted CD4$^+$ T cells[44]. Thus, PD-L1/L2 upregulation in monocytes may be critical for tumor formation and progression through not only CD8$^+$ T cell but also CD4$^+$ T cell suppression (Figure 7).

A previous study also showed that TAMs near the HRS cells had higher PD-L1 expression than TAMs that were distant from HRS cells[14]. Although cytokines, such as interferon-gamma (IFN-γ) and granulocyte-macrophage colony-stimulating factors, secreted by HRS cells can be considered as reasons for PD-L1 enhancement[14, 45-48], the detailed mechanism underlying the upregulation of PD-L1 in TAMs proximal to HRS cells remained elusive. Here, we suggest trogocytosis as one of the mechanisms behind increased PD-L1/L2 expression in TAMs near HRS cells.

Our *in vitro* study demonstrated that co-culture with L-1236 cells upregulated PD-L1/L2 in monocytes in only one hour (Figure 2). Due to early upregulation, we focused on trogocytosis, which is known as protein transfer from one cell to another[29-31]. Since trogocytosis is a rapid direct protein delivery system distinguished from humoral factors, such as cytokines and exosomes, it results in an early increase in protein levels in the recipient cells[29]. Indeed, our confocal microscopy study confirmed the movement of PD-L1/L2 from HRS cells to monocytes (Figure 3). The contribution of trogocytosis in the

rapid upregulation of PD-L1/L2 was further verified when co-culture with L-1236^{L1L2KO} did not affect PD-L1/L2 expression in monocytes (Figure 4A, B) and that with L-428$^{L1/L2+OE}$ or L-428$^{L1/L2++OE}$ significantly upregulated PD-L1/L2 expression in monocytes, in a dose-dependent manner (Figure 4C, D and Supplemental Figure 6). Thus, the rapid upregulation of PD-L1/L2 on monocyte cell surfaces primarily originated from trogocytosis.

Trogocytosis occurs *in vitro* and *in vivo*, and its function may be important in immune response regulation[29]. For instance, the acquisition of MHC class II molecules by natural killer cells from dendritic cells leads to the inhibition of $CD4^+$ T cell-mediated immune regulation[32]. Another study revealed that CD86 transfer from inducible regulatory T cells to dendritic cells augmented immune suppression[49]. Furthermore, in cHL, CD137 transition from HRS cells to APCs was involved in immune evasion by inhibiting T cell activation[50]. Indeed, our *in vitro* qPCR and ELISA analysis showed that PD-L1 on THP-1 cells acquired from HRS cells have an inhibitory effect on $CD3^+$ T cells (Figure 5). Taken together, the transfer of PD-L1/L2 from HRS cells to monocytes might relate to the establishment of TIME in cHL through T cell suppression.

To validate trogocytosis-mediated PD-L1/L2 transfer from HRS cells to TAMs in cHL patients, we examined human tissue specimens of cHL. A previous study using multiple fluorescence staining in 20 cHL samples demonstrated that PD-L1 upregulation was observed in TAMs near HRS cells rather than in TAMs distant from HRS cells, whereas

328 PD-L2 expression in TAMs responded to their distance from HRS cells, and the PD-L1/L2
329 levels on TAMs in direct contact with HRS cells remained unknown[14]. In this study, we
330 performed double immunofluorescence staining on 38 cHL samples. Both PD-L1 and PD-L2
331 expression were higher in TAMs in contact with HRS cells compared with TAMs distant from
332 HRS cells (Figure 6). Based on pathologists' quantification, proximity to HRS cells affected
333 PD-L1 expression in TAMs, where TAMs that were closest to HRS had higher PD-L1
334 expression levels (HRS-contacted > HRS-close > HRS-distant). In contrast, there was no
335 obvious correlation between PD-L2 expression in TAMs and the distance between TAMs
336 and HRS cells. In addition, although software quantification showed that both PD-L1 and
337 PD-L2 on HRS-close TAMs were elevated compared to HRS-distant TAMs, the difference in
338 PD-L2 expression (%) between HRS-close and HRS-distant TAMs was small compared to
339 the difference in PD-L1 expression (%) between HRS-close and HRS-distant TAMs
340 (Supplemental Figure 10). One possible reason is that PD-L2 expression is generally lower
341 than PD-L1 expression in HRS cells (Supplemental Table 3 and Supplemental Figure 9).
342 This is also reported in previous immunostaining studies where PD-L1 was markedly
343 expressed while PD-L2 was generally weakly positive in HRS cells[51, 52]. Moreover, taking
344 into account our *in vitro* results where the level of protein transfer is dependent on the
345 PD-L1/L2 expression levels on HRS cells, less PD-L2 may be transferred from HRS cells to
346 TAMs compared to PD-L1.

PD-L1/L2 on TAMs in direct contact with the HRS cells may also be elevated by humoral factors secreted by HRS cells. Indeed, our *in vitro* analysis revealed that the supernatants from a few particular HRS cell cultures increased PD-L1/L2 on monocytes (Supplemental Figure 2). Still, trogocytosis seems to be another efficient mechanism since we observed that CD30 expression was also elevated in monocytes that were in contact with HRS cells (Figure 6C). Although humoral factors may elevate TAM expression of PD-L1/L2 in some cases of cHL, trogocytosis is an additional potential mechanism for PD-L1/L2 elevation on TAMs in cHL patients, which leads to T cell suppression by the MHC pathway.

Thus, inhibition of PD-L1/L2 upregulation on monocytes is a potential therapeutic target for cHL. Blocking the interaction between a chemokine and its receptor is a rational strategy for inhibition of direct contact between cells, which is necessary for trogocytosis. Indeed, a recent study using a CCR5 antagonist that prevented the recruitment of monocytes in tumor tissues was able to inhibit tumor progression with low toxicity in HRS-xenograft mice[53]. Further studies are required to determine the efficacy of inhibition of direct contact between cells.

In conclusion, PD-L1 and PD-L2 expression levels in monocytes newly recruited to tumor tissues were elevated via trogocytosis from HRS cells, which may contribute to the upregulation of PD-L1/L2 in TAMs near HRS cells. Trogocytosis was more effective in facilitating the rapid increase of PD-L1/L2 on the cell surface of TAMs compared to humoral

366 factors. We hypothesize that trogocytosis-mediated PD-L1/L2 transfer from HRS cells
367 suppresses effector T cells through the PD-1 and PD-L1/L2 axis by MHC presentation.
368
369 **Acknowledgements** The authors thank Chisa Okada, Kazuhiro Yoshida, Yoshinori
370 Okada, Hiromi Iida, Yudai Kawai, and the Support Center for Medical Research and
371 Education, as well as Tokai University for technical assistance.
372
373 **Funding** This research was supported by The Jikei University Research Fund for
374 Graduate Students to M.Kawashima; Precursory Research for Embryonic Science and
375 Technology, AMED-PRIME to A.K.; the Research Program on Hepatitis from the Japan
376 Agency for Medical Research and Development (19fk0210054s0201), the Core Research
377 for Evolutional Science and Technology (CREST) of the Japan, and the Uehara Memorial
378 Foundation to A.K.
379
380 **Author contribution** M. Kawashima, H.H., R.K., T.H., K.O., N.S., M. Kakizaki, Y.M., K.A.,
381 M.N., S.U., R.H., Y.H., K.K., S.G., T.K., K.C., S.Y. and A.K. performed the experiments
382 shown in this study. J.C. and N.N. carried out immunostaining and evaluated the slides of
383 cHL patients. M. Kawashima performed all other experiments and statistical analysis; M.
384 Kawashima and A.K. wrote the manuscript; A.K. edited the manuscript drafts.

Compliance with ethical standards

Conflict-of-interest The authors have no conflicts of interest to disclose.

Reference

1. Swerdlow SH, Campo E, Harris N, Jaffe ES, Pileri SA, Stein H, *et al.* WHO Classification of Tumours of Haematopoietic and Lymphoid Tissues (Revised 4th edition). 2017: Lyon: IARC;.

2. Aldinucci D, Gloghini A, Pinto A, De Filippi R, Carbone A. The classical Hodgkin's lymphoma microenvironment and its role in promoting tumour growth and immune escape. *The Journal of Pathology* 2010; **221**(3): 248–263.

3. Steidl C, Connors JM, Gascoyne RD. Molecular pathogenesis of Hodgkin's lymphoma: increasing evidence of the importance of the microenvironment. *J Clin Oncol* 2011 May 10; **29**(14): 1812–1826.

4. Kuppers R, Engert A, Hansmann ML. Hodgkin lymphoma. *J Clin Invest* 2012 Oct; **122**(10): 3439–3447.

5. Steidl C, Lee T, Shah SP, Farinha P, Han G, Nayar T, *et al.* Tumor–associated macrophages and survival in classic Hodgkin's lymphoma. *N Engl J Med* 2010 Mar 11; **362**(10): 875–885.

6. Tan KL, Scott DW, Hong F, Kahl BS, Fisher RI, Bartlett NL, *et al.* Tumor–associated macrophages predict inferior outcomes in classic Hodgkin lymphoma: a correlative study from the E2496 Intergroup trial. *Blood* 2012; **120**(16): 3280–3287.

7. Guo B, Cen H, Tan X, Ke Q. Meta–analysis of the prognostic and clinical value of tumor–associated macrophages in adult classical Hodgkin lymphoma. *BMC Med* 2016 Oct 17; **14**(1): 159.

8. Tadmor T, Bari A, Marcheselli L, Sacchi S, Aviv A, Baldini L, *et al.* Absolute Monocyte Count and Lymphocyte–Monocyte Ratio Predict Outcome in Nodular Sclerosis Hodgkin Lymphoma: Evaluation Based on Data From 1450 Patients. *Mayo Clin Proc* 2015 Jun; **90**(6): 756–764.

9. Porrata LF, Ristow K, Colgan JP, Habermann TM, Witzig TE, Inwards DJ, *et al.* Peripheral blood lymphocyte/monocyte ratio at diagnosis and survival in classical Hodgkin's lymphoma. *Haematologica* 2012 Feb; **97**(2): 262–269.

10. Skinnider BF. The role of cytokines in classical Hodgkin lymphoma. *Blood* 2002; **99**(12): 4283–4297.

11. Ma Y, Visser L, Roelofsen H, de Vries M, Diepstra A, van Imhoff G*, et al.* Proteomics analysis of Hodgkin lymphoma: identification of new players involved in the cross-talk between HRS cells and infiltrating lymphocytes. *Blood* 2008 Feb 15; **111**(4): 2339–2346.

12. Peyraud F, Cousin S, Italiano A. CSF-1R Inhibitor Development: Current Clinical Status. *Curr Oncol Rep* 2017 Sep 5; **19**(11): 70.

13. von Tresckow B, Morschhauser F, Ribrag V, Topp MS, Chien C, Seetharam S*, et al.* An Open-Label, Multicenter, Phase I/II Study of JNJ-40346527, a CSF-1R Inhibitor, in Patients with Relapsed or Refractory Hodgkin Lymphoma. *Clin Cancer Res* 2015 Apr 15; **21**(8): 1843–1850.

14. Carey CD, Gusenleitner D, Lipschitz M, Roemer MGM, Stack EC, Gjini E*, et al.* Topological analysis reveals a PD-L1-associated microenvironmental niche for Reed-Sternberg cells in Hodgkin lymphoma. *Blood* 2017 Nov 30; **130**(22): 2420–2430.

15. Yamamoto R, Nishikori M, Kitawaki T, Sakai T, Hishizawa M, Tashima M*, et al.* PD-1-PD-1 ligand interaction contributes to immunosuppressive microenvironment of Hodgkin lymphoma. *Blood* 2008 Mar 15; **111**(6): 3220–3224.

16. Green MR, Monti S, Rodig SJ, Juszczynski P, Currie T, O'Donnell E*, et al.* Integrative analysis reveals selective 9p24.1 amplification, increased PD-1 ligand expression, and further induction via JAK2 in nodular sclerosing Hodgkin lymphoma and primary mediastinal large B-cell lymphoma. *Blood* 2010; **116**(17): 3268–3277.

17. Roemer MG, Advani RH, Ligon AH, Natkunam Y, Redd RA, Homer H*, et al.* PD-L1 and PD-L2 Genetic Alterations Define Classical Hodgkin Lymphoma and Predict Outcome. *J Clin Oncol* 2016 Aug 10; **34**(23): 2690–2697.

18. Ansell SM, Lesokhin AM, Borrello I, Halwani A, Scott EC, Gutierrez M*, et al.* PD-1 blockade with nivolumab in relapsed or refractory Hodgkin's lymphoma. *N Engl J Med* 2015 Jan 22; **372**(4): 311–319.

19. Younes A, Santoro A, Shipp M, Zinzani PL, Timmerman JM, Ansell S*, et al.* Nivolumab for classical Hodgkin's lymphoma after failure of both autologous stem-cell transplantation and

brentuximab vedotin: a multicentre, multicohort, single-arm phase 2 trial. *The Lancet Oncology* 2016 Sep; **17**(9): 1283-1294.

20. Armand P, Shipp MA, Ribrag V, Michot JM, Zinzani PL, Kuruvilla J*, et al.* Programmed Death-1 Blockade With Pembrolizumab in Patients With Classical Hodgkin Lymphoma After Brentuximab Vedotin Failure. *J Clin Oncol* 2016 Nov 1; **34**(31): 3733-3739.

21. Chen R, Zinzani PL, Fanale MA, Armand P, Johnson NA, Brice P*, et al.* Phase II Study of the Efficacy and Safety of Pembrolizumab for Relapsed/Refractory Classic Hodgkin Lymphoma. *J Clin Oncol* 2017 Jul 1; **35**(19): 2125-2132.

22. Herbaux C, Gauthier J, Brice P, Drumez E, Ysebaert L, Doyen H*, et al.* Efficacy and tolerability of nivolumab after allogeneic transplantation for relapsed Hodgkin lymphoma. *Blood* 2017 May 4; **129**(18): 2471-2478.

23. Kuang DM, Zhao Q, Peng C, Xu J, Zhang JP, Wu C*, et al.* Activated monocytes in peritumoral stroma of hepatocellular carcinoma foster immune privilege and disease progression through PD-L1. *J Exp Med* 2009 Jun 8; **206**(6): 1327-1337.

24. Lau J, Cheung J, Navarro A, Lianoglou S, Haley B, Totpal K*, et al.* Tumour and host cell PD-L1 is required to mediate suppression of anti-tumour immunity in mice. *Nat Commun* 2017 Feb 21; **8**: 14572.

25. Lin H, Wei S, Hurt EM, Green MD, Zhao L, Vatan L*, et al.* Host expression of PD-L1 determines efficacy of PD-L1 pathway blockade-mediated tumor regression. *J Clin Invest* 2018 Feb 1; **128**(2): 805-815.

26. Yearley JH, Gibson C, Yu N, Moon C, Murphy E, Juco J*, et al.* PD-L2 Expression in Human Tumors: Relevance to Anti-PD-1 Therapy in Cancer. *Clin Cancer Res* 2017 Jun 15; **23**(12): 3158-3167.

27. Chen BJ, Chapuy B, Ouyang J, Sun HH, Roemer MG, Xu ML*, et al.* PD-L1 expression is characteristic of a subset of aggressive B-cell lymphomas and virus-associated malignancies. *Clin Cancer Res* 2013 Jul 1; **19**(13): 3462-3473.

28. Vari F, Arpon D, Keane C, Hertzberg MS, Talaulikar D, Jain S*, et al.* Immune evasion via PD-1/PD-L1 on NK cells and monocyte/macrophages is more prominent in Hodgkin lymphoma than DLBCL. *Blood* 2018 Apr 19; **131**(16): 1809-1819.

29. Davis DM. Intercellular transfer of cell-surface proteins is common and can affect many stages of an immune response. *Nat Rev Immunol* 2007 Mar; **7**(3): 238-243.

30. Ahmed KA, Munegowda MA, Xie Y, Xiang J. Intercellular trogocytosis plays an important role in modulation of immune responses. *Cellular & molecular immunology* 2008 Aug; **5**(4): 261-269.

31. Nakayama M. Antigen Presentation by MHC-Dressed Cells. *Front Immunol* 2014; **5**: 672.

32. Nakayama M, Takeda K, Kawano M, Takai T, Ishii N, Ogasawara K. Natural killer (NK)-dendritic cell interactions generate MHC class II-dressed NK cells that regulate CD4+ T cells. *Proc Natl Acad Sci U S A* 2011 Nov 8; **108**(45): 18360-18365.

33. Roda-Navarro P, Reyburn HT. Intercellular protein transfer at the NK cell immune synapse: mechanisms and physiological significance. *FASEB journal : official publication of the Federation of American Societies for Experimental Biology* 2007 Jun; **21**(8): 1636-1646.

34. Trambas CM, Griffiths GM. Delivering the kiss of death. *Nat Immunol* 2003 May; **4**(5): 399-403.

35. Kreiter S, Vormehr M, van de Roemer N, Diken M, Lower M, Diekmann J*, et al.* Mutant MHC class II epitopes drive therapeutic immune responses to cancer. *Nature* 2015 Apr 30; **520**(7549): 692-696.

36. Linnemann C, van Buuren MM, Bies L, Verdegaal EM, Schotte R, Calis JJ*, et al.* High-throughput epitope discovery reveals frequent recognition of neo-antigens by CD4+ T cells in human melanoma. *Nat Med* 2015 Jan; **21**(1): 81-85.

37. Ott PA, Hu Z, Keskin DB, Shukla SA, Sun J, Bozym DJ*, et al.* An immunogenic personal neoantigen vaccine for patients with melanoma. *Nature* 2017 Jul 13; **547**(7662): 217-221.

38. Reichel J, Chadburn A, Rubinstein PG, Giulino-Roth L, Tam W, Liu Y*, et al.* Flow sorting and exome sequencing reveal the oncogenome of primary Hodgkin and Reed-Sternberg cells. *Blood* 2015 Feb 12; **125**(7): 1061-1072.

39. Roemer MGM, Redd RA, Cader FZ, Pak CJ, Abdelrahman S, Ouyang J*, et al.* Major Histocompatibility Complex Class II and Programmed Death Ligand 1 Expression Predict

Outcome After Programmed Death 1 Blockade in Classic Hodgkin Lymphoma. *J Clin Oncol* 2018 Apr 1; **36**(10): 942–950.

40. Tumeh PC, Harview CL, Yearley JH, Shintaku IP, Taylor EJ, Robert L, *et al.* PD-1 blockade induces responses by inhibiting adaptive immune resistance. *Nature* 2014 Nov 27; **515**(7528): 568–571.

41. Im SJ, Hashimoto M, Gerner MY, Lee J, Kissick HT, Burger MC, *et al.* Defining CD8+ T cells that provide the proliferative burst after PD-1 therapy. *Nature* 2016 Sep 15; **537**(7620): 417–421.

42. Wein F, Kuppers R. The role of T cells in the microenvironment of Hodgkin lymphoma. *J Leukoc Biol* 2016 Jan; **99**(1): 45–50.

43. Wein F, Weniger MA, Hoing B, Arnolds J, Huttmann A, Hansmann ML, *et al.* Complex Immune Evasion Strategies in Classical Hodgkin Lymphoma. *Cancer Immunol Res* 2017 Dec; **5**(12): 1122–1132.

44. Cader FZ, Schackmann RCJ, Hu X, Wienand K, Redd R, Chapuy B, *et al.* Mass cytometry of Hodgkin lymphoma reveals a CD4(+) regulatory T-cell-rich and exhausted T-effector microenvironment. *Blood* 2018 Aug 23; **132**(8): 825–836.

45. Keir ME, Butte MJ, Freeman GJ, Sharpe AH. PD-1 and its ligands in tolerance and immunity. *Annu Rev Immunol* 2008; **26**: 677–704.

46. Garcia-Diaz A, Shin DS, Moreno BH, Saco J, Escuin-Ordinas H, Rodriguez GA, *et al.* Interferon Receptor Signaling Pathways Regulating PD-L1 and PD-L2 Expression. *Cell Rep* 2017 May 9; **19**(6): 1189–1201.

47. Mimura K, Teh JL, Okayama H, Shiraishi K, Kua LF, Koh V, *et al.* PD-L1 expression is mainly regulated by interferon gamma associated with JAK-STAT pathway in gastric cancer. *Cancer Sci* 2018 Jan; **109**(1): 43–53.

48. Thorn M, Guha P, Cunetta M, Espat NJ, Miller G, Junghans RP, *et al.* Tumor-associated GM-CSF overexpression induces immunoinhibitory molecules via STAT3 in myeloid-suppressor cells infiltrating liver metastases. *Cancer gene therapy* 2016 Jun; **23**(6): 188–198.

49. Gu P, Gao JF, D'Souza CA, Kowalczyk A, Chou KY, Zhang L. Trogocytosis of CD80 and CD86 by induced regulatory T cells. *Cellular & molecular immunology* 2012 Mar; **9**(2): 136-146.

50. Ho WT, Pang WL, Chong SM, Castella A, Al-Salam S, Tan TE, *et al.* Expression of CD137 on Hodgkin and Reed-Sternberg Cells Inhibits T-cell Activation by Eliminating CD137 Ligand Expression. *Cancer Research* 2012; **73**(2): 652-661.

51. Panjwani PK, Charu V, DeLisser M, Molina-Kirsch H, Natkunam Y, Zhao S. Programmed death-1 ligands PD-L1 and PD-L2 show distinctive and restricted patterns of expression in lymphoma subtypes. *Hum Pathol* 2018 Jan; **71**: 91-99.

52. Tanaka Y, Maeshima AM, Nomoto J, Makita S, Fukuhara S, Munakata W, *et al.* Expression pattern of PD-L1 and PD-L2 in classical Hodgkin lymphoma, primary mediastinal large B-cell lymphoma, and gray zone lymphoma. *Eur J Haematol* 2018 May; **100**(5): 511-517.

53. Casagrande N, Borghese C, Visser L, Mongiat M, Colombatti A, Aldinucci D. CCR5 antagonism by maraviroc inhibits Hodgkin lymphoma microenvironment interactions and xenograft growth. *Haematologica* 2019 Mar; **104**(3): 564-575.

Figure Legends

Figure 1. Monocytes migrate towards and come into direct contact with HRS cell lines.

(A) Monocytes in contact with L-591-mOrange$^+$ or L-1236-mOrange$^+$ in semi-solid cultures. Three independent experiments were carried out, and representative data are shown. scale bar: 10 μm, original magnification ×20. (B) The number of HRS-mOrange$^+$ cells (L-591 and L-1236) that migrated to monocytes was counted in the transwell cultures. (C) The number of CD14$^+$ monocytes that migrated to the wells with the supernatant of HRS cells was counted (L-591: left, L-1236; right). CCL19 (10 nM) or CCL2 (100 ng/ml) was used as the positive control (PC), and RPMI1640 medium was the negative control (NC). Migration index indicates the cell number in each sample divided by that in the NC. (n = 3). Error bar: mean ± SD. *P < 0.05, **P < 0.01, N.S.: not significant. The data were analyzed by Student's t-test.

Figure 2. PD-L1/L2 expression was rapidly upregulated in monocytes by direct contact with HRS cells.

(A) Representative plots show the gating strategy for flow cytometry. HRS-mOrange$^+$ and PI$^+$ cells were excluded, then CD14$^+$ biotin-streptavidin binding monocytes were gated for further analysis (red rectangle). (B)(C) Histogram of PD-L1/L2 on monocytes with HRS cells and supernatant (sup) of the cells are shown. (B) MFI (PD-L1/PD-L2); control: 61.2/5.4,

without HRS cells: 411/5.9, with L-1236 sup: 418/5.88, with L-1236 mix: 808/69, *Positive cells (PD-L1/PD-L2); without HRS cells: 32.3%/3.44%, with L-1236 sup: 32%/3.2%, with L-1236 cells: 71.9%/72.6%. (C) MFI (PD-L1/PD-L2); control: 54.2/5.31, without HRS cells: 241/7.3, with L-591 sup: 275/7.67, with L-591 cells: 432/7.6, with L-428 sup: 297/6.43, with L-428 cells: 320/9.64. *Positive cells (PD-L1/PD-L2); without HRS cells: 15.4%/0.54%, with L-591 sup: 20.7%/0.69%, with L-591 cells 46.6%/0.97%, with L-428 sup: 22.8%/0.5%, with L-428 cells: 28.6%/1.46%. (D) After monocytes were cultured with PD-L1/L2 overexpressing L-428 (L-428$^{L1/L2++OE}$) or control (L-428^{Vector}) for five minutes, expression of PD-L1/L2 on monocytes was analyzed by flow cytometry. MFI (PD-L1/PD-L2); control: 136/7.87, without HRS cells: 267/8.93, with L-428$^{L1/L2++OE}$: 1078/561, *Positive cells (PD-L1/PD-L2); without HRS cells: 5.55%/0.09%, with L-428$^{L1/L2++OE}$: 49.1%/89.7%. Three experiments were performed, and representative data are presented.

Figure 3. PD-L1/L2 were transferred from HRS cells to monocytes.

(A) PKH26-labeled L-1236 cells (red) and PKH67-labeled (green) monocytes were co-cultured. (B)(C) L-1236 or L-428 cells stained for PD-L1 (blue) and PD-L2 (red) were mixed with PKH67-labeled monocytes. Nuclei of monocytes were also labeled with Hoechst 33258 (White). (C) Co-localization of PD-L1/L2 with monocytes denoted white. Figures indicate PD-L1/monocytes (upper) and PD-L2/monocytes (lower). Scale bar: 10 μm; original

636 magnification ×40. (D) Expression levels of PD-L1/L2 and CD30 were compared between
637 L-1236, L-591, and L-428 cells by flow cytometry. MFI (PD-L1/PD-L2/CD30); L-591 (control):
638 14.2/13.6/43.8, L-1236 (control): 22.5/19.5/124, L-428 (control): 18/13.5/51.5, L-591:
639 155/39.8/24489, L-1236:1462/1082/1145, L-428: 135/126/29726. *Positive cells
640 (PD-L1/PD-L2/CD30); L-591: 32.5%/14.8%/99.4%, L-1236: 99.3%/98.9%/27.2%, L-428:
641 30.5%/68.7%/99.4%. (E) CD30 (blue) stained L-428 cells were co-cultured with
642 PKH67-labeled monocytes. Scale bar: 10 μm; original magnification ×40. (F) CD30
643 expression on monocytes after one hour of co-culture with HRS cells was measured by flow
644 cytometry. MFI; control: 24, without HRS cells: 27.2, with L-1236 sup: 38.8, with L-1236
645 cells: 71.7, with L-591 sup: 33.3, with L-591 cells: 487, with L-428 sup: 29.8, with L-428 cells:
646 2151. *Positive cells; without HRS cells: 1.69%, with L-1236 sup: 1.45%, with L-1236 cells:
647 7.82%, with L-591 sup: 2.49%, with L-591 cells 43.8%, with L-428 sup: 2.03%, with L-428
648 cells: 86.2%. Each analysis was performed three times, and representatives are shown.
649
650 **Figure 4. Expression of PD-L1/L2 on monocytes was unchanged in co-cultures with**
651 **PD-L1/L2-deficient HRS cells.**
652 (A) Expression of PD-L1/L2 on PD-L1/L2-deficient L-1236 cells (L-1236$^{L1/L2KO}$) and control
653 vector cells (L-1236^{Vector}). MFI (PD-L1/PD-L2); L-1236 $^{L1/L2KO}$ (control): 19.5/31, L-1236^{Vector}
654 (control): 18.9/27.9, L-1236$^{L1/L2KO}$: 91.4/63.4, L-1236^{Vector}: 2534/1348. *Positive cells

655 (PD-L1/PD-L2); L-1236^{KO}: 14.5%/1.81%, L-1236^{Vector}: 99.8%/97.2%. (B) After monocytes

656 were cultured with L-1236$^{L1/L2KO}$ or L-1236^{Vector} for one hour, expression of PD-L1/L2 and

657 CD30 on monocytes were analyzed by flow cytometry. MFI (PD-L1/PD-L2/CD30); control:

658 35.4/5.04/33.4, without HRS cells: 206/6.29/36.3, with L-1236$^{L1/L2KO}$: 193/8.24/60.1, with

659 L-1236^{Vector}: 583/121/59.8, *Positive cells (PD-L1/PD-L2/CD30); without HRS cells:

660 21.2%/0.08%/3.02%, with L-1236$^{L1/L2KO}$: 19.5%/0.39%/6.55%, with L-1236^{Vector}:

661 86.7%/72.5%/6.74%. (C) Expression of PD-L1/L2 on two PD-L1/L2-overexpression cells

662 (L-428$^{L1/L2++OE}$) and control vector cells (L-428^{Vector}). MFI (PD-L1/PD-L2); L-428^{Vector}

663 (control): 13.9/10.6, L-428$^{L1/L2++OE}$ (control): 13.1/8.83, L-428^{Vector}: 62.1/128, L-428$^{L1/L2++OE}$:

664 8077/2889. *Positive cells (PD-L1/PD-L2): L-428^{Vector} (10.5%/70.7%), L-428$^{L1/L2++OE}$

665 (99.4%/99.8%). (D) After monocytes were cultured with L-428$^{L1/L2++OE}$ or L-428^{Vector} for one

666 hour, expression of PD-L1/L2 on monocytes was analyzed by flow cytometry. MFI

667 (PD-L1/PD-L2); control: 54.3/8.5. without HRS cells: 119/6.99, with L-428^{Vector}: 147/8.5, with

668 L-428$^{L1/L2++OE}$: 747/358, *Positive cells (PD-L1/PD-L2); without HRS cells: 6.17%/0.06%,

669 with L-428^{Vector}: 11.2%/0.33%, with L-428$^{L1/L2++OE}$: 75.3%/90.1%. The experiments were

670 performed in triplicate, and representative histograms are presented.

671

672 **Figure 5. PD-L1 on THP-1 cells from HRS cells has an inhibitory effect on T cells.**

673 (A)(B) THP-1 cells were co-cultured with L-428^{Vector} or L-428^{L1++OE} for one hour, and then
674 THP-1 cells were isolated, respectively (THP-1 (trogL-428^{Vector}) or THP-1 (trogL-428^{L1++OE}).
675 Purified CD3^{+} T cells were pre-stimulated by anti-CD3 antibody 1 μg/ml for 24 hours.
676 Post-stimulated CD3^{+} cells were co-cultured with THP-1 (trogL-428^{Vector}) or THP-1
677 (trogL-428^{L1++OE}) for two hours at a ratio of 2:1. (A) Total RNA was collected for co-cultured
678 cells or CD3^{+} T cells. CD69, IL-2, or IFN-γ expression was measured by qPCR. (B) The cell
679 culture supernatant was collected, and IFN-γ secretion was measured by ELISA. mRNA of
680 CD69, IL-2, and IFN-γ and secretion of IFN-γ from THP-1 (trogL-428^{Vector}) and THP-1
681 (trogL-428^{L1++OE}) cells was undetectable (data not shown). Error bar: mean ± SD. *P < 0.05,
682 **P < 0.01. The data were analyzed by Student's t-test. These data are representative of
683 three independent experiments.
684
685 **Figure 6. Expression of PD-L1 and PD-L2 on TAMs in contact with HRS cells were**
686 **higher than in TAMs distant from HRS cells in cHL patients.**
687 (A) Analysis procedures are briefly shown**.** (I) TAMs near the HRS area were determined by
688 CD30 staining. The CD30-abundant region was defined as the HRS^{+} area, and the
689 CD30-scarce region was defined as the HRS^{-} area (each area: 130 μm × 170 μm). Brown:
690 CD30. TAMs were further classified as follows: (1) HRS-contacted: the distance from
691 macrophages to CD30-positive HRS cells is within 5 μm in HRS^{+} area (and most of the

692 macrophages are in direct physical contact with HRS cells); (2) HRS-close: the distance
693 from macrophages to CD30-positive HRS cells is within 110 μm in HRS^+ area; and (3)
694 HRS-distant: the macrophages that are not close to HRS cells in HRS^- area. (II) Next,
695 PD-L1/CD163 and PD-L2/CD163 double staining were performed in each area. Brown:
696 PD-L1/L2; red: CD163. (B) PD-L1/L2 expression on TAMs among HRS-contacted,
697 HRS-close, and HRS-distant were measured, and boxplots represent the data. The boxes
698 denote the median, and the first and third quartile; the upper and lower whiskers represent
699 the 90% and 10%, respectively (N = 38). The Friedman's test was performed, and
700 Bonferroni correction was used for multiple comparisons. *P < 0.01, ** P < 0.001. N.S.: not
701 significant. (C) Representative immunostaining images of CD30 on the HRS^+ area are
702 shown. HRS cells and macrophages that express CD30 are highlighted by squares. Brown:
703 CD30. Scale bar: 20 μm, Original magnification ×400.
704
705 **Figure 7. Schema for the tumor microenvironment in cHL.**
706 I. Monocytes from peripheral blood are recruited by HRS cells into the tumor
707 microenvironment and differentiate into TAMs. Within a short period of time, trogocytosis
708 from HRS cells to TAMs occurs by direct contact, resulting in rapid upregulation of PD-L1/L2
709 on the surface of TAMs. II. PD-L1 and PD-L2 elevation on cell surfaces of TAMs near HRS
710 cells suppress effector T cells through PD-1 and PD-L1/L2 interaction by MHC presentation.

711 This contributes to the tumor's escape from immune surveillance, leading to the progression

712 of the tumor microenvironment.

Figure 1

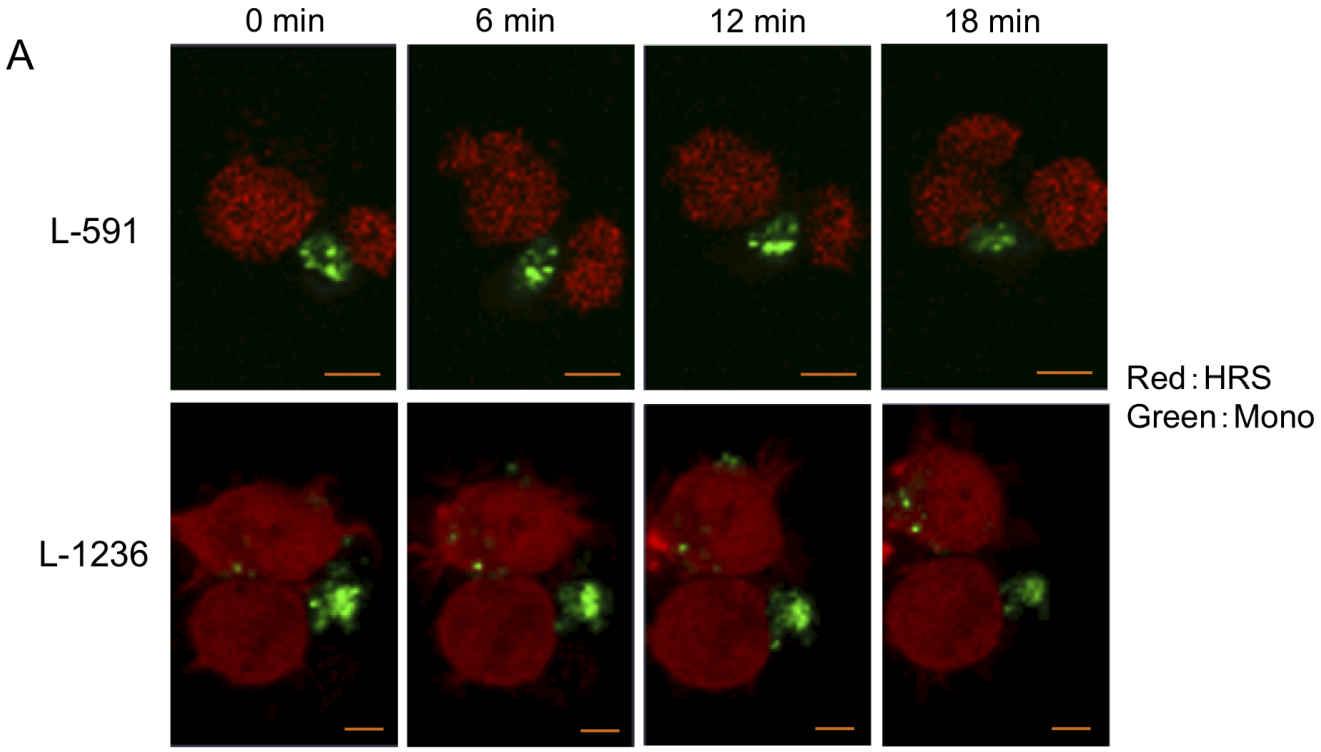
A
0 min
6 min
12 min
18 min
L-591
L-1236
Red : HRS
Green : Mono

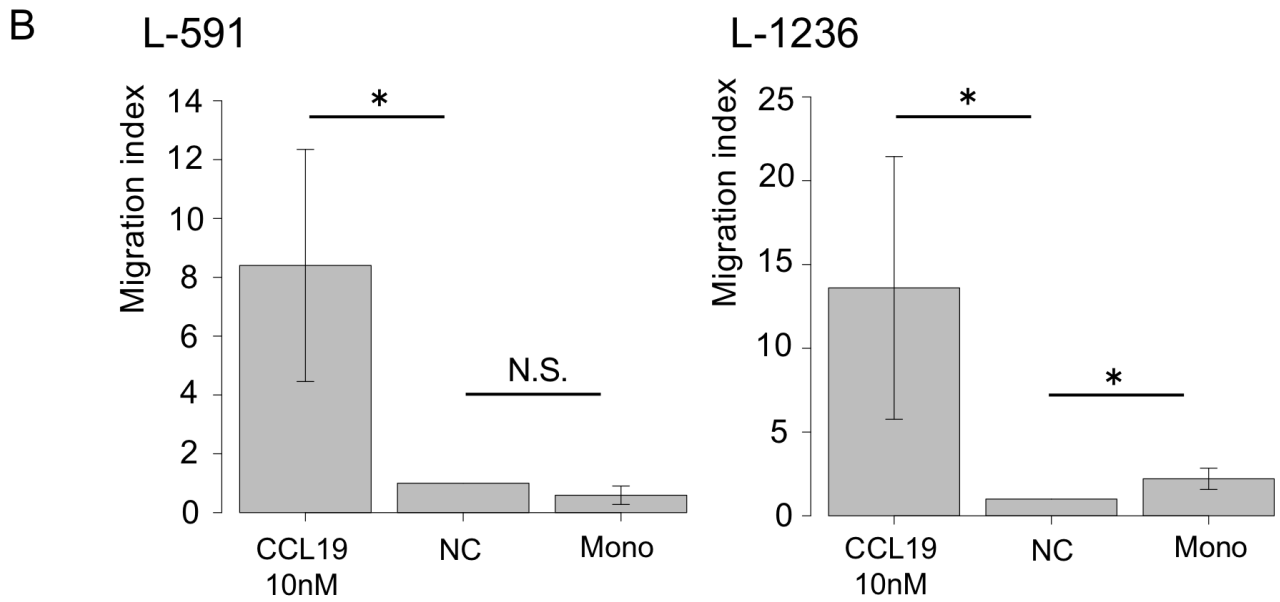
B
L-591
L-1236
Migration index
*
N.S.
CCL19
10nM
NC
Mono

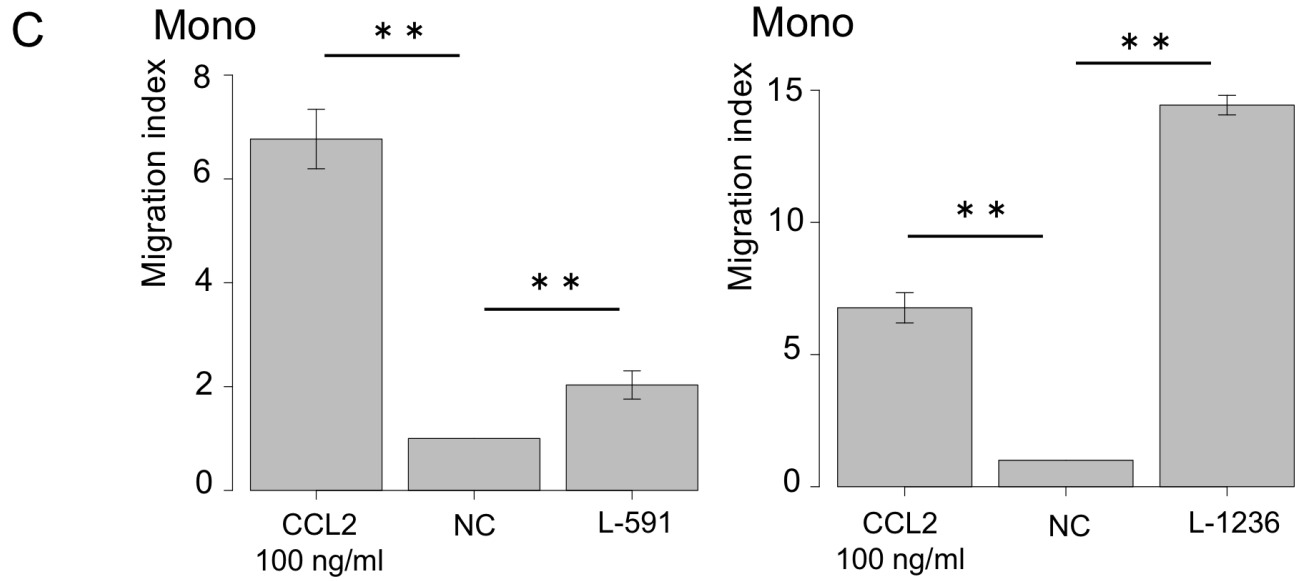
C
Mono
Mono
Migration index
* *
CCL2
100 ng/ml
NC
L-591
L-1236

Figure 2

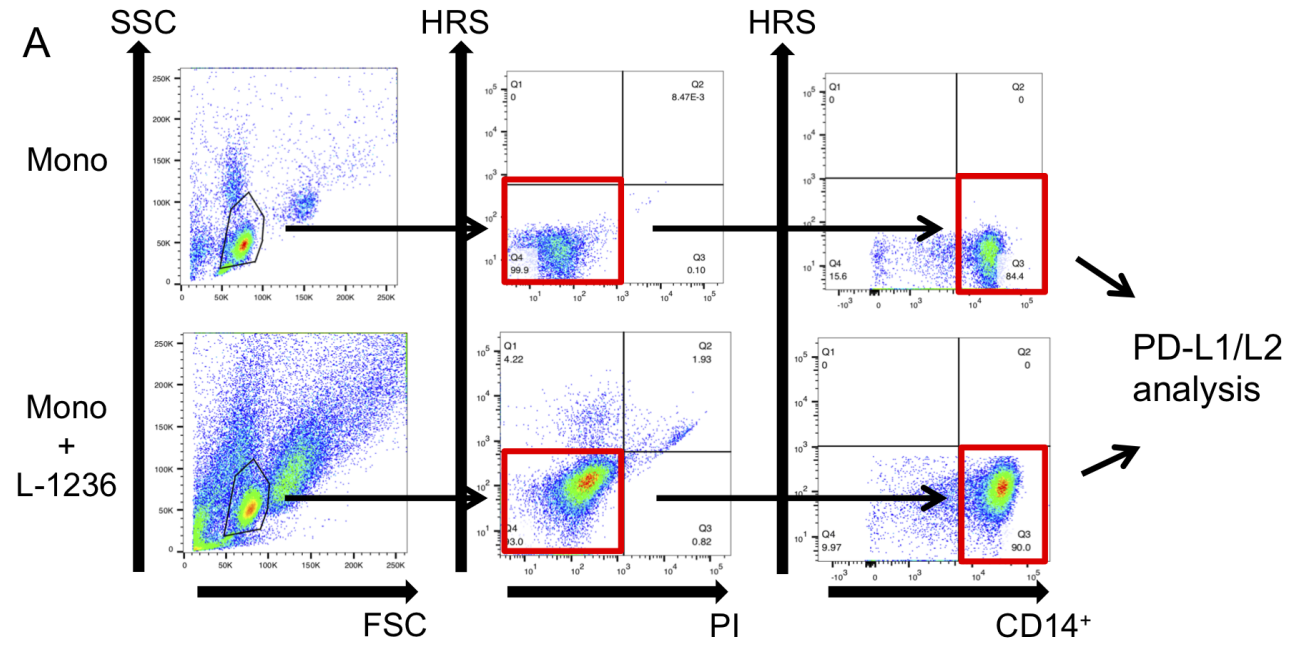
A
SSC
HRS
HRS
Mono
Mono
+
L-1236
PD-L1/L2
analysis
FSC
PI
CD14+

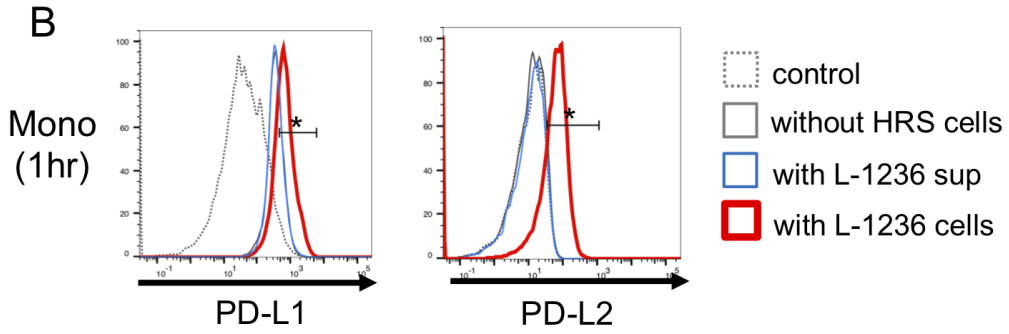
B
Mono
(1hr)
PD-L1
PD-L2
control
without HRS cells
with L-1236 sup
with L-1236 cells

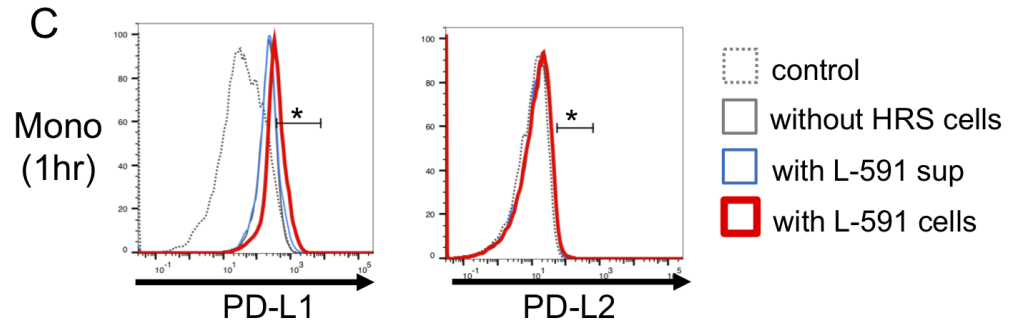
C
Mono
(1hr)
PD-L1
PD-L2
control
without HRS cells
with L-591 sup
with L-591 cells

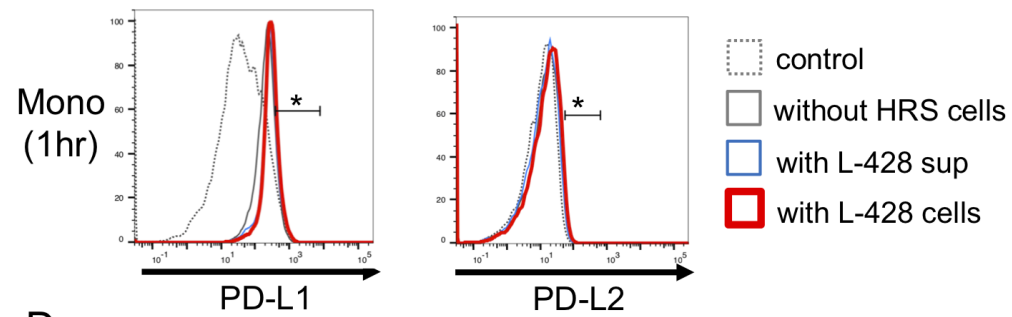
Mono
(1hr)
PD-L1
PD-L2
control
without HRS cells
with L-428 sup
with L-428 cells

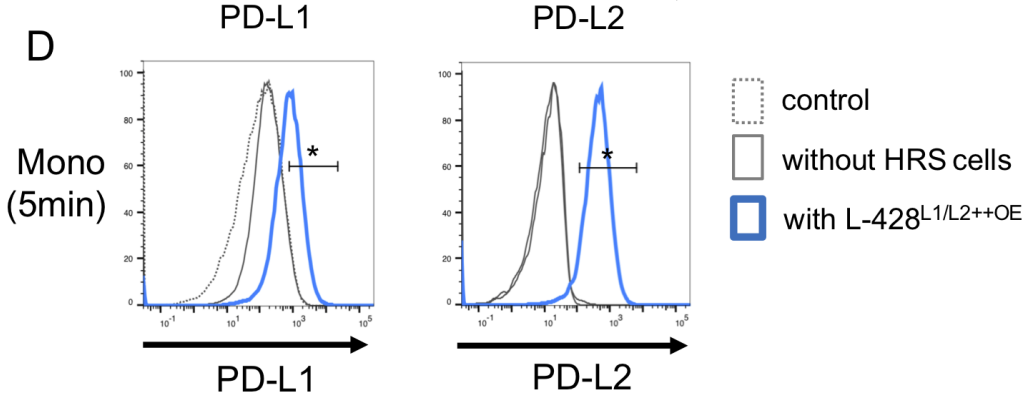
D
Mono
(5min)
PD-L1
PD-L2
control
without HRS cells
with L-428L1/L2++OE

Figure 3

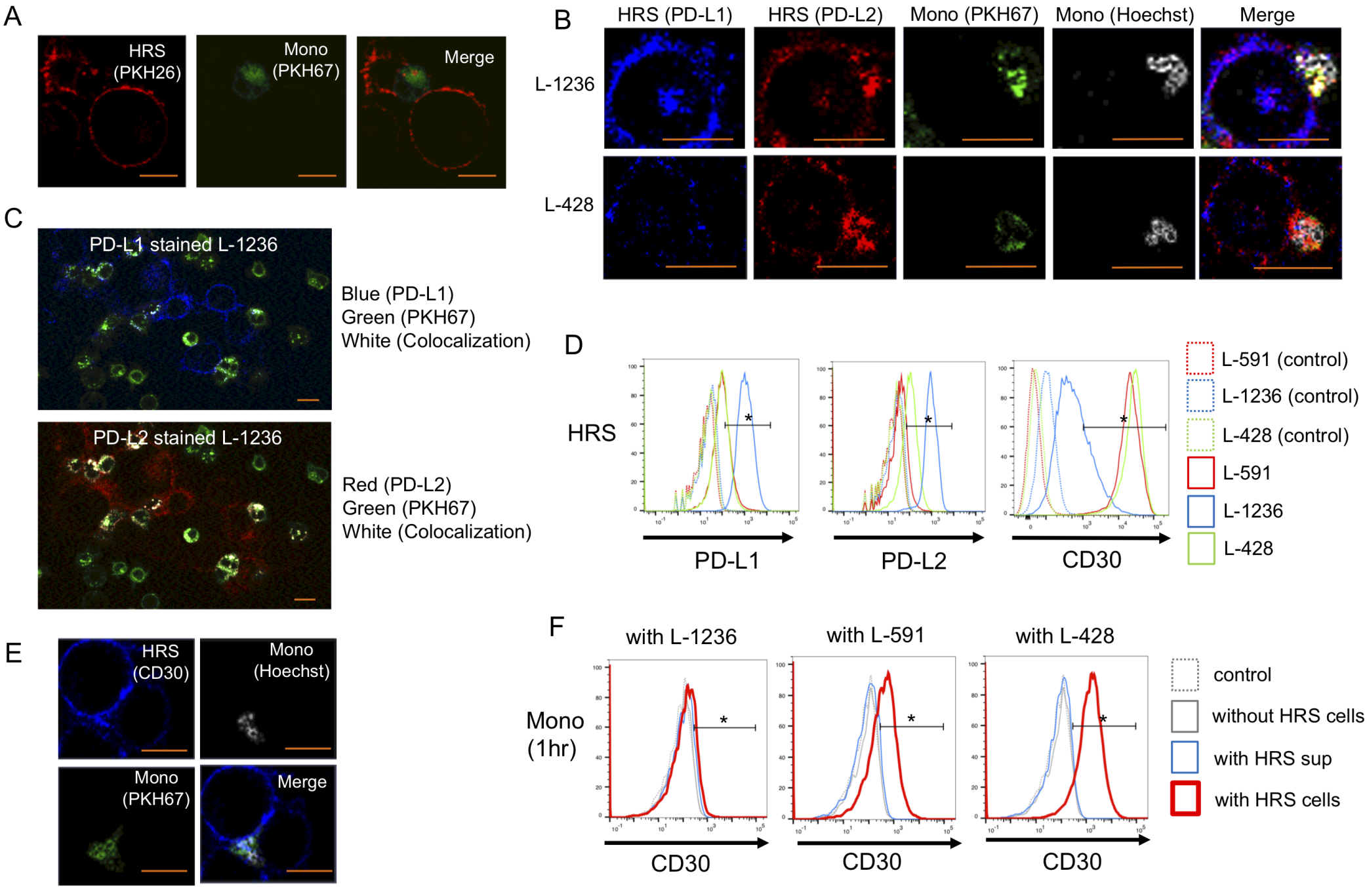
A
HRS (PKH26)
Mono (PKH67)
Merge
B
HRS (PD-L1)
HRS (PD-L2)
Mono (PKH67)
Mono (Hoechst)
Merge
L-1236
L-428
C
PD-L1 stained L-1236
Blue (PD-L1)
Green (PKH67)
White (Colocalization)
PD-L2 stained L-1236
Red (PD-L2)
Green (PKH67)
White (Colocalization)
D
HRS
PD-L1
PD-L2
CD30
L-591 (control)
L-1236 (control)
L-428 (control)
L-591
L-1236
L-428
E
HRS (CD30)
Mono (Hoechst)
Mono (PKH67)
Merge
F
with L-1236
with L-591
with L-428
Mono (1hr)
CD30
CD30
CD30
control
without HRS cells
with HRS sup
with HRS cells

Figure 4

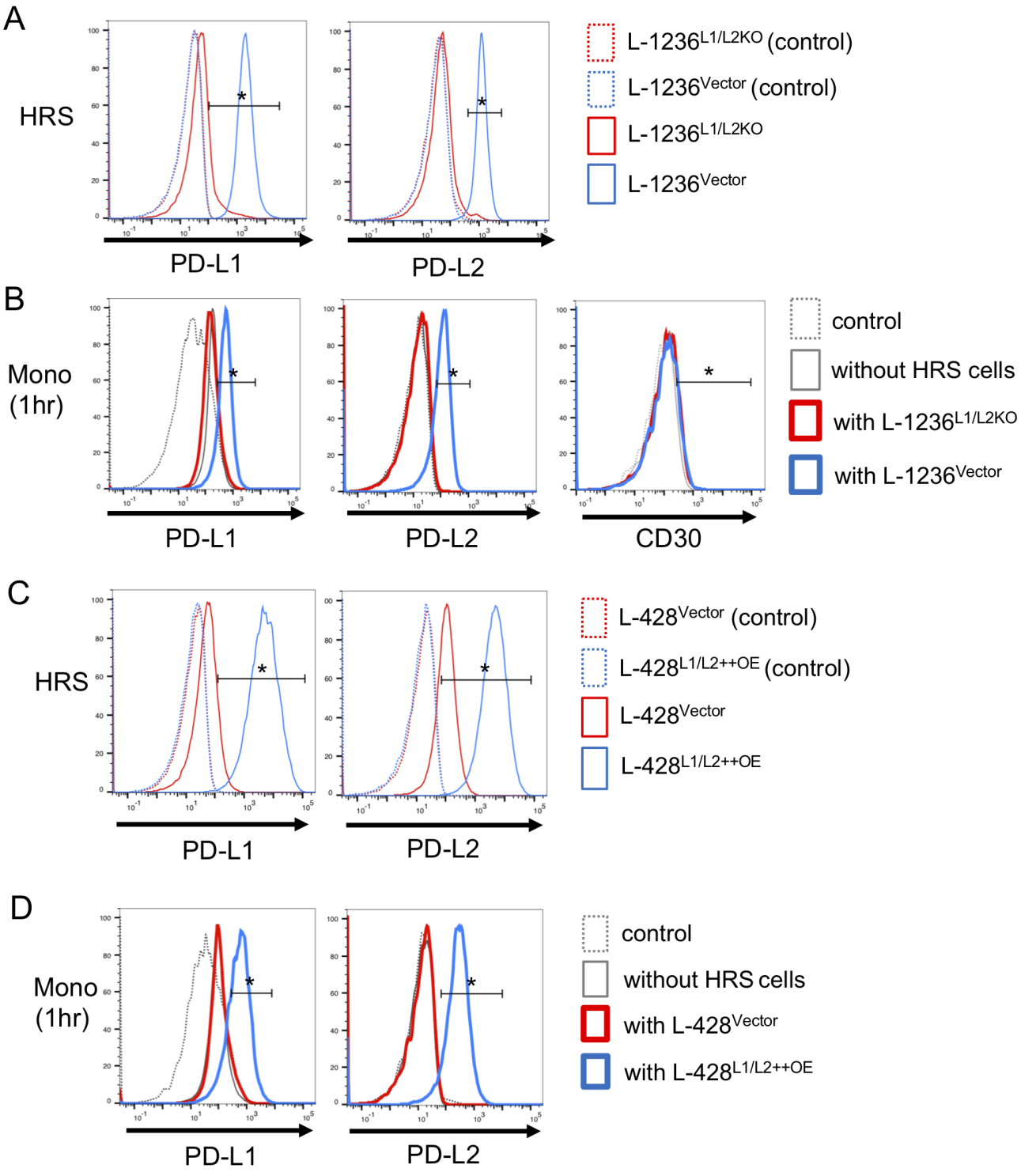
A
HRS
PD-L1
PD-L2
L-1236L1/L2KO (control)
L-1236Vector (control)
L-1236L1/L2KO
L-1236Vector
B
Mono (1hr)
PD-L1
PD-L2
CD30
control
without HRS cells
with L-1236L1/L2KO
with L-1236Vector
C
HRS
PD-L1
PD-L2
L-428Vector (control)
L-428L1/L2++OE (control)
L-428Vector
L-428L1/L2++OE
D
Mono (1hr)
PD-L1
PD-L2
control
without HRS cells
with L-428Vector
with L-428L1/L2++OE

Figure 5

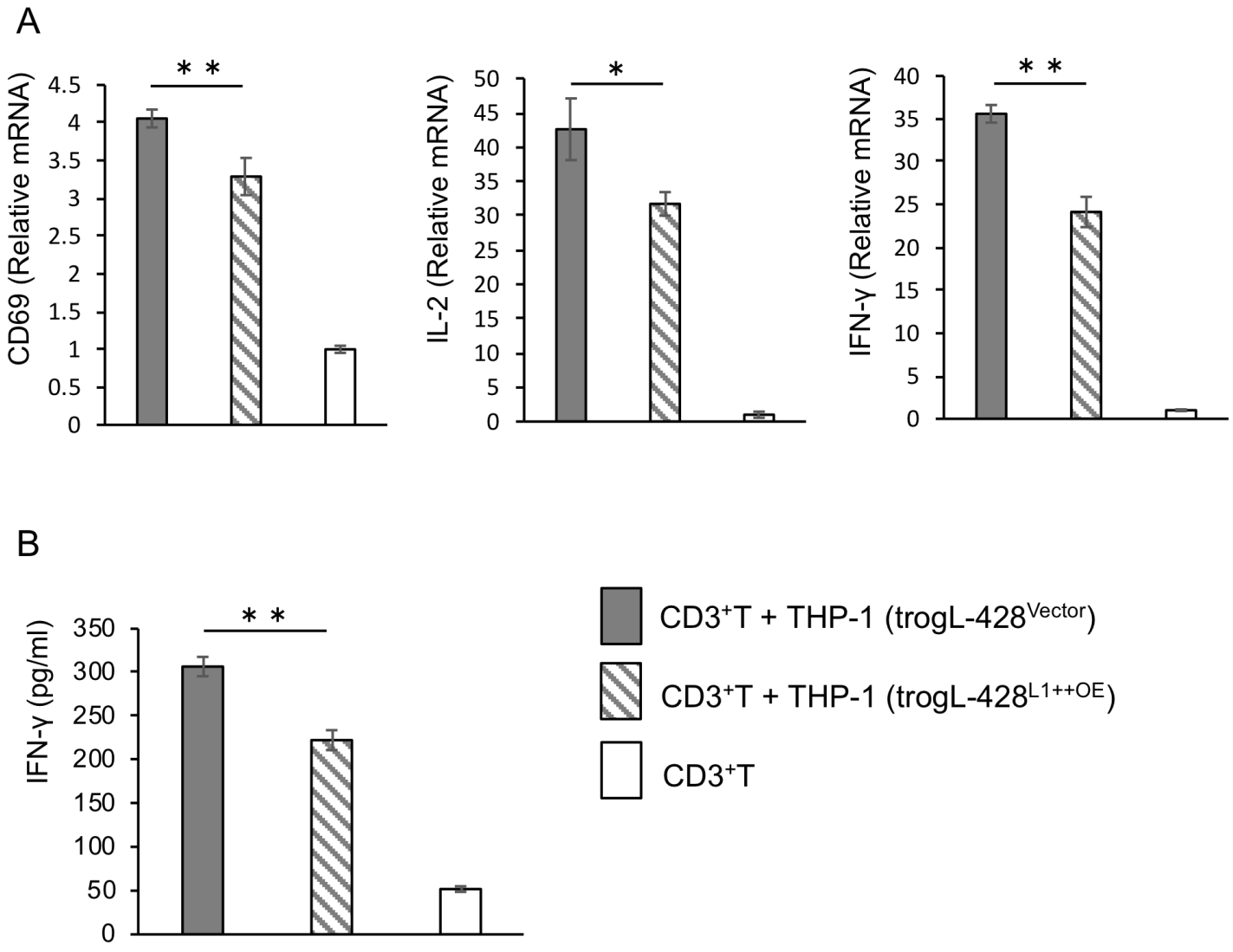
A
CD69 (Relative mRNA)
IL-2 (Relative mRNA)
IFN-γ (Relative mRNA)
* *
*
* *
B
IFN-γ (pg/ml)
* *
CD3+T + THP-1 (trogL-428Vector)
CD3+T + THP-1 (trogL-428L1++OE)
CD3+T

Figure 6

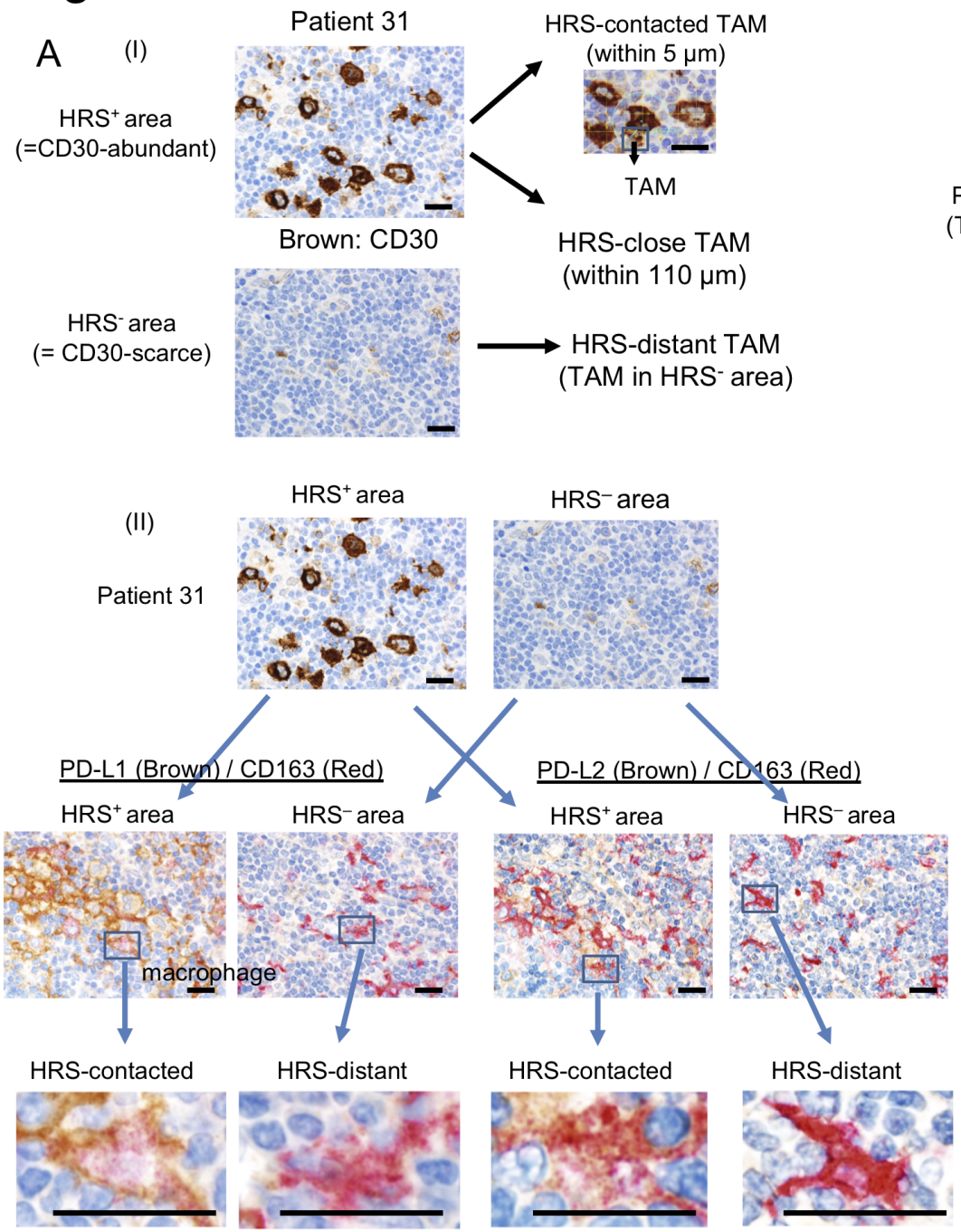
A
(I)
Patient 31
HRS+ area
(=CD30-abundant)
HRS-contacted TAM
(within 5 μm)
TAM
HRS-close TAM
(within 110 μm)
Brown: CD30
HRS- area
(= CD30-scarce)
HRS-distant TAM
(TAM in HRS- area)
(II)
Patient 31
HRS+ area
HRS− area
PD-L1 (Brown) / CD163 (Red)
PD-L2 (Brown) / CD163 (Red)
HRS+ area
HRS− area
HRS+ area
HRS− area
macrophage
HRS-contacted
HRS-distant
HRS-contacted
HRS-distant

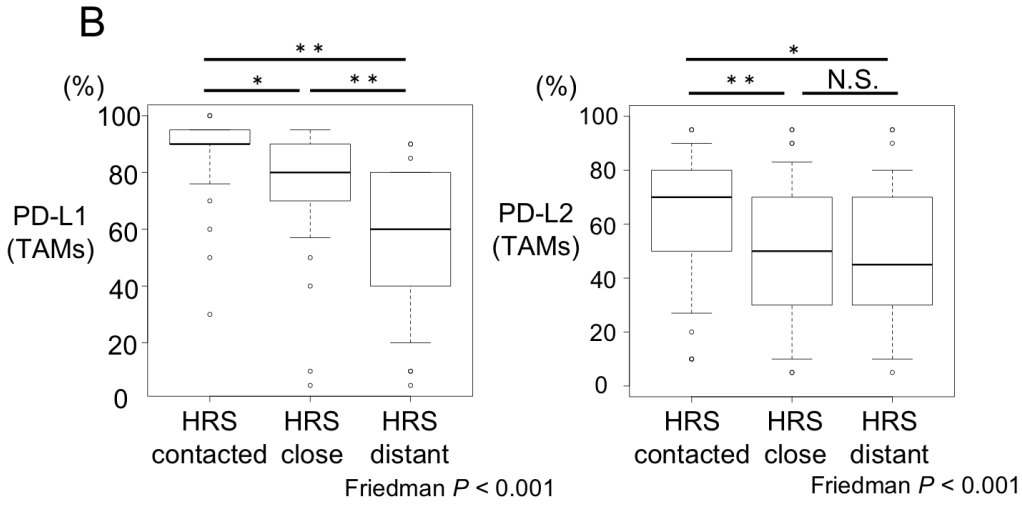
B
(%)
PD-L1
(TAMs)
100
80
60
40
20
0
HRS
contacted
HRS
close
HRS
distant
Friedman P < 0.001
(%)
PD-L2
(TAMs)
N.S.
Friedman P < 0.001

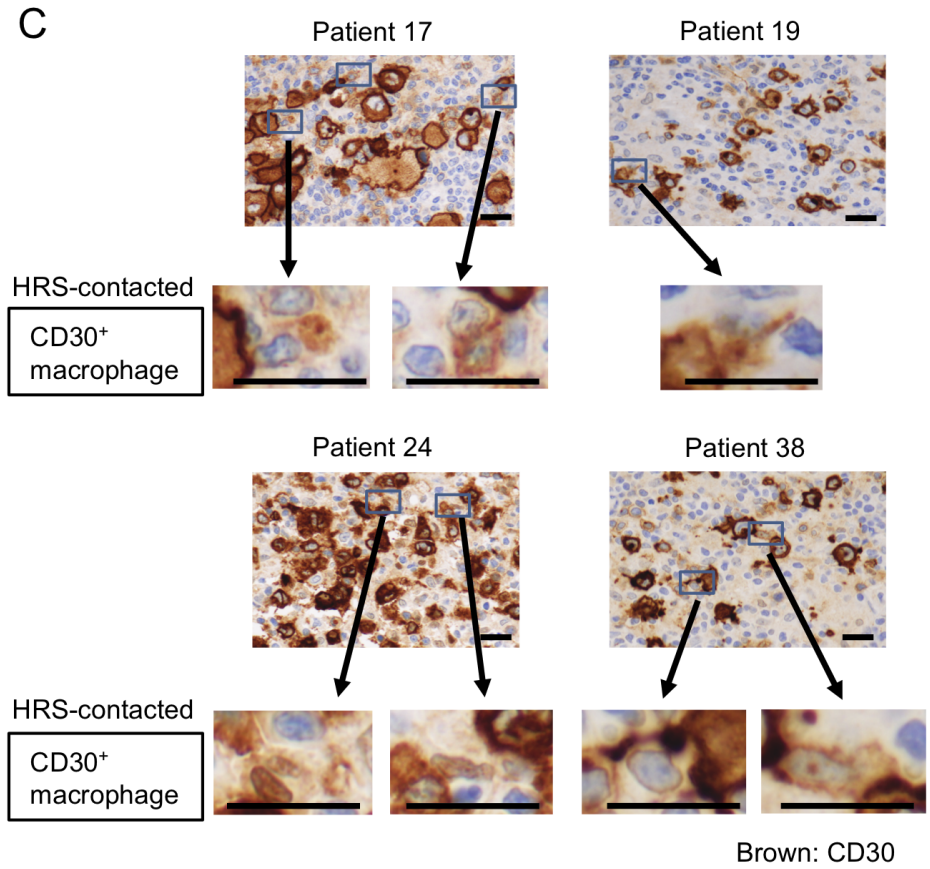
C
Patient 17
Patient 19
HRS-contacted
CD30+
macrophage
Patient 24
Patient 38
HRS-contacted
CD30+
macrophage
Brown: CD30

Figure 7

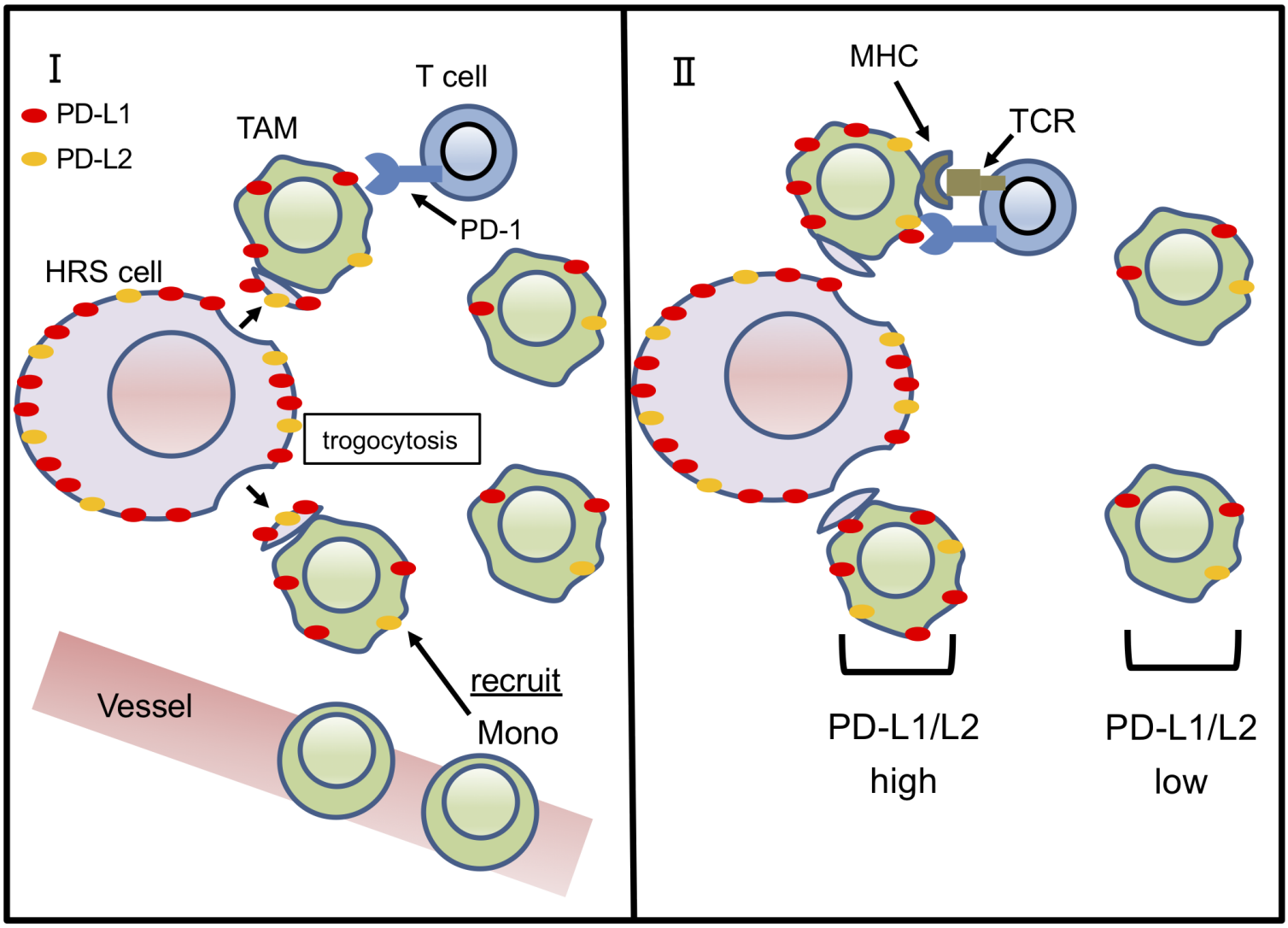
I
PD-L1
PD-L2
T cell
TAM
PD-1
HRS cell
trogocytosis
recruit
Mono
Vessel
II
MHC
TCR
PD-L1/L2
high
PD-L1/L2
low

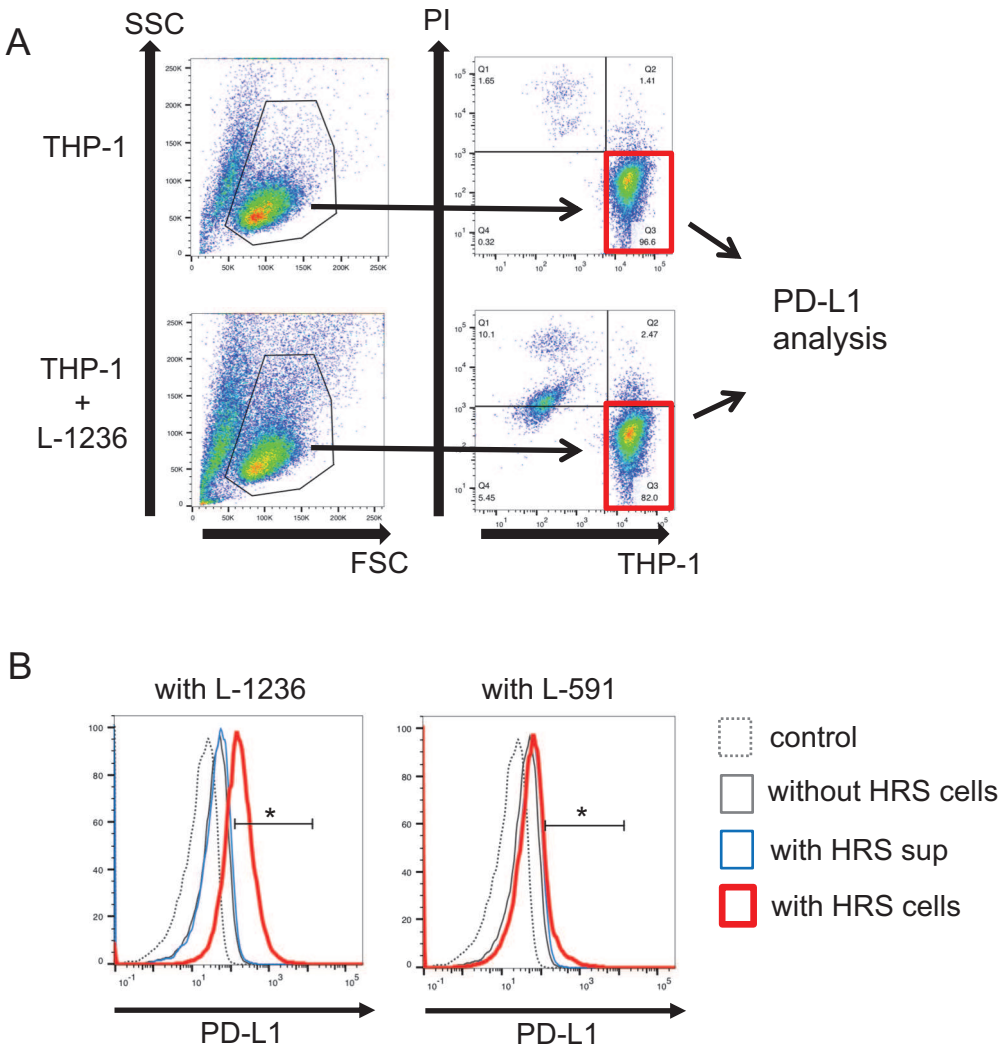

Supplemental Figure 1. Increase protein levels of PD-L1 on THP-1-Venus$^+$ co-cultured with L-1236 cells.

1×10^5 THP-1-Venus$^+$ cells and/or 1×10^5 HRS cells were cultured in a 24-well plate for 6 hours. (A) Representative plots show the gating strategy for flow cytometry. PI$^+$ cells were excluded and THP-1-Venus$^+$ fractions were gated for further analysis (red rectangle). (B) Histogram of PD-L1 on THP-1 with HRS cells and supernatant (sup) of the cells are shown. MFI; control: 11.9, without HRS cells: 44.5, with L-1236 sup; 50.5, with L-1236 cells; 262, with L-591 sup; 58.2, with L-591 cells 101. *Positive cells; without HRS cells: 4.42%, with L-1236 sup: 7.24%, with L-1236 cells: 69.2%, with L-591 sup: 9.87%, with L-591 cells: 18.7%. Three experiments were performed, and representative data are presented.

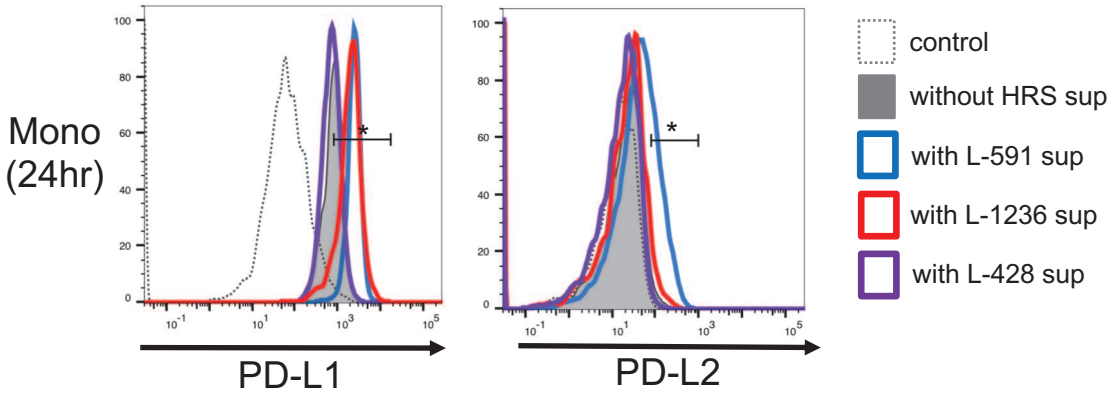

Supplemental Figure 2. Supernatant of some HRS cell lines elevated PD-L1/L2 on monocytes for 24-hour cultured conditions.

5 $\times 10^5$ PBMCs were cultured with supernatant (sup) of each HRS cell lines in a 24-well plate for 24 hours. PI^+ cells were excluded and $CD14^+$ biotin-streptavidin stained monocytes fractions were analyzed. Histograms are presented. MFI (PD-L1/PD-L2); control: 162/8.8, without HRS sup: 881/16.6, with L-591 sup: 2574/53.8, with L-1236 sup: 2263/21.3, with L-428 sup: 807/12.4. *Positive cells (PD-L1/PD-L2); without HRS sup: 49.5%/1.86%, with L-591 sup: 98.1%/22.5%, with L-1236 sup: 88.9%/3.86%, with L-428 sup: 39.3%/0.71%. Experiments were repeated at three times, and the representative data are shown.

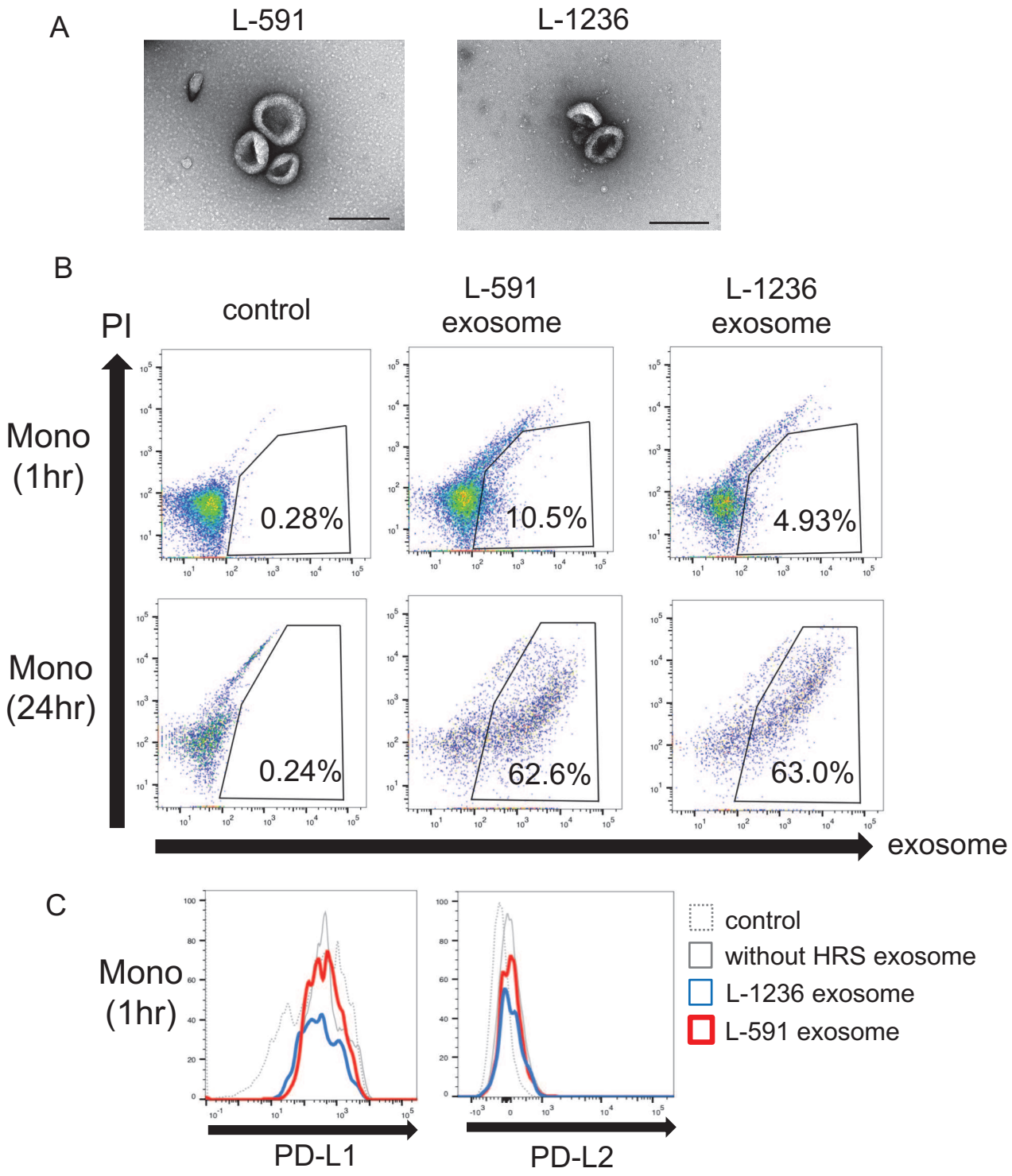

Supplemental Figure 3. Only a small amount of purified exosomes of HRS cell lines were incorporated into monocytes for one hour treatment.
(A) Purified exosomes were observed by transmission electron microscope. Scale bar: 200 nm, (B) Monocytes were treated with PKH26 labeled 5 μg/ml exosomes of HRS cell lines in one hour and 24 hours, then FACS analysis was performed. (C) PD-L1/L2 on the monocytes which incorporated the $PKH^{+}PI^{-}$ exosomes were analyzed by FACS. The representative of two data are shown.

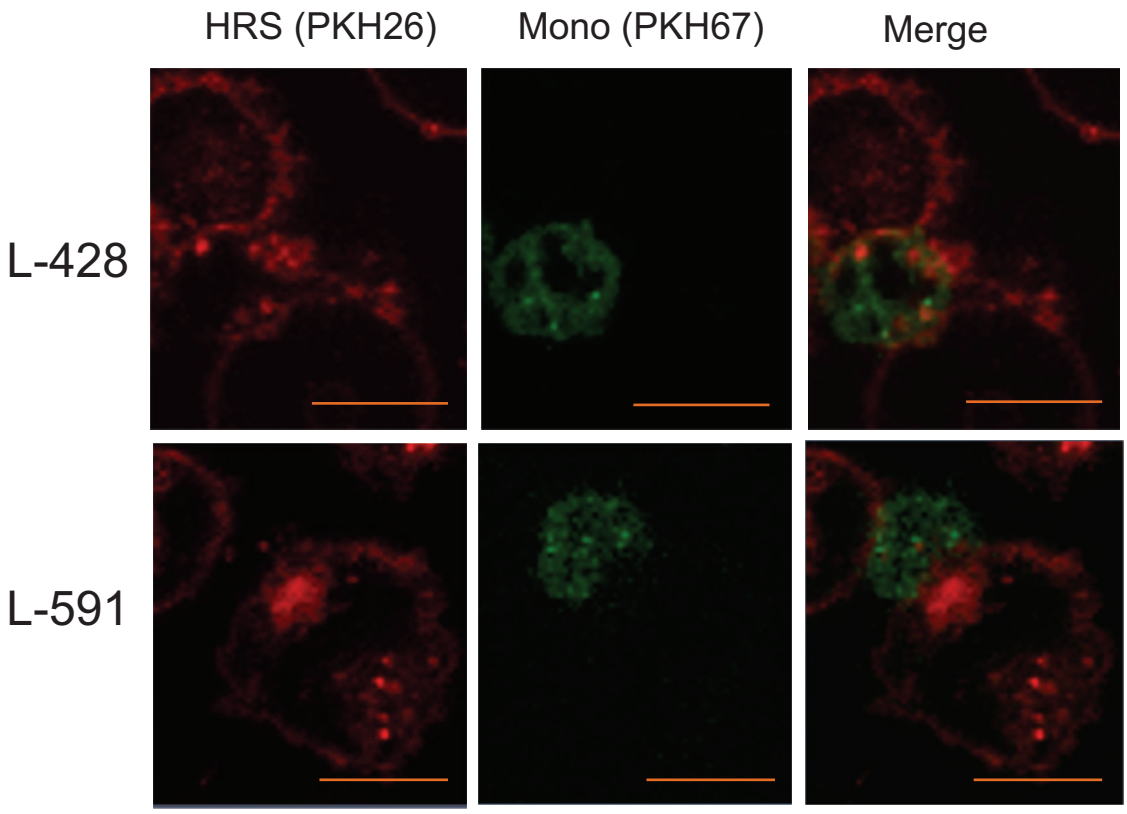

Supplemental Figure 4. Trogocytosis also occurred from L-428/L-591 to monocytes. PKH26-labeled (red) L-428 or L-591 cells were co-cultured with PKH67-labeled (green) monocytes. Scale bar: 10 μm; original magnification ×40. Representative figures of three independent experiments are shown.

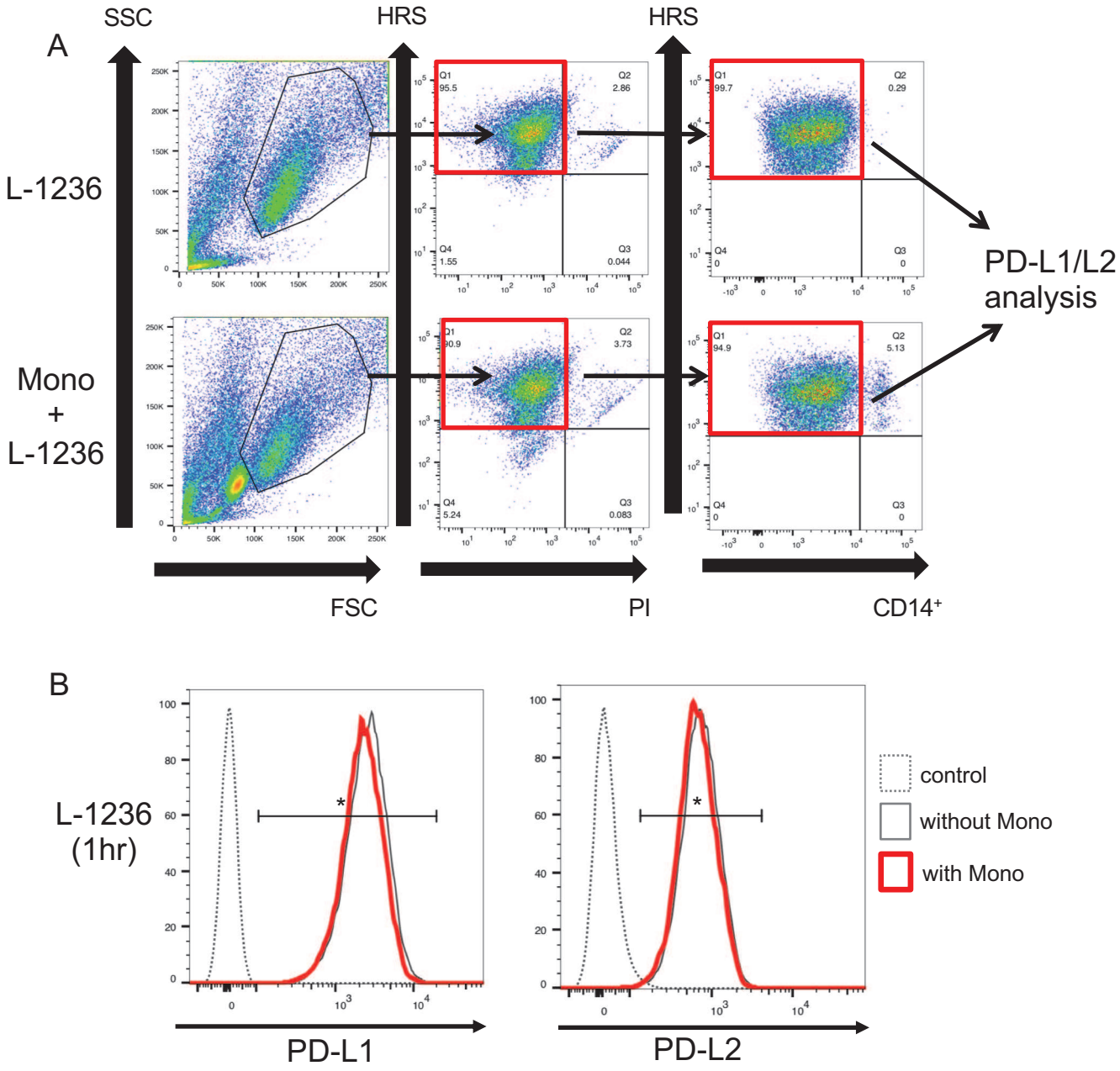

Supplemental Figure 5. PD-L1/L2 expression in L-1236 cultured with monocytes were not largely decreased.

L-1236-mOrange$^+$ cells were cultured with monocytes or without in one hour, and then FACS analysis was performed. (A) Representative plots show the gating strategy for flow cytometry. PI$^-$ and HRS-mOrange$^+$ fractions were gated. Subsequently, CD14$^+$ biotin-streptavidin binding monocytes were excluded and red rectangle fractions was analyzed. (B) Gating demonstrated that PD-L1/L2 on L-1236-mOrange$^+$ cultured with monocytes were not largely downregulated compared to these without monocytes. MFI (PD-L1/PD-L2); control: 9.97/26.1, without Mono: 2935/830, with Mono: 2633/769. *Positive cells (PD-L1/PD-L2): without Mono; 99.9%/99.7%, with Mono: 100%/99.6%. The data are representative of three experiments.

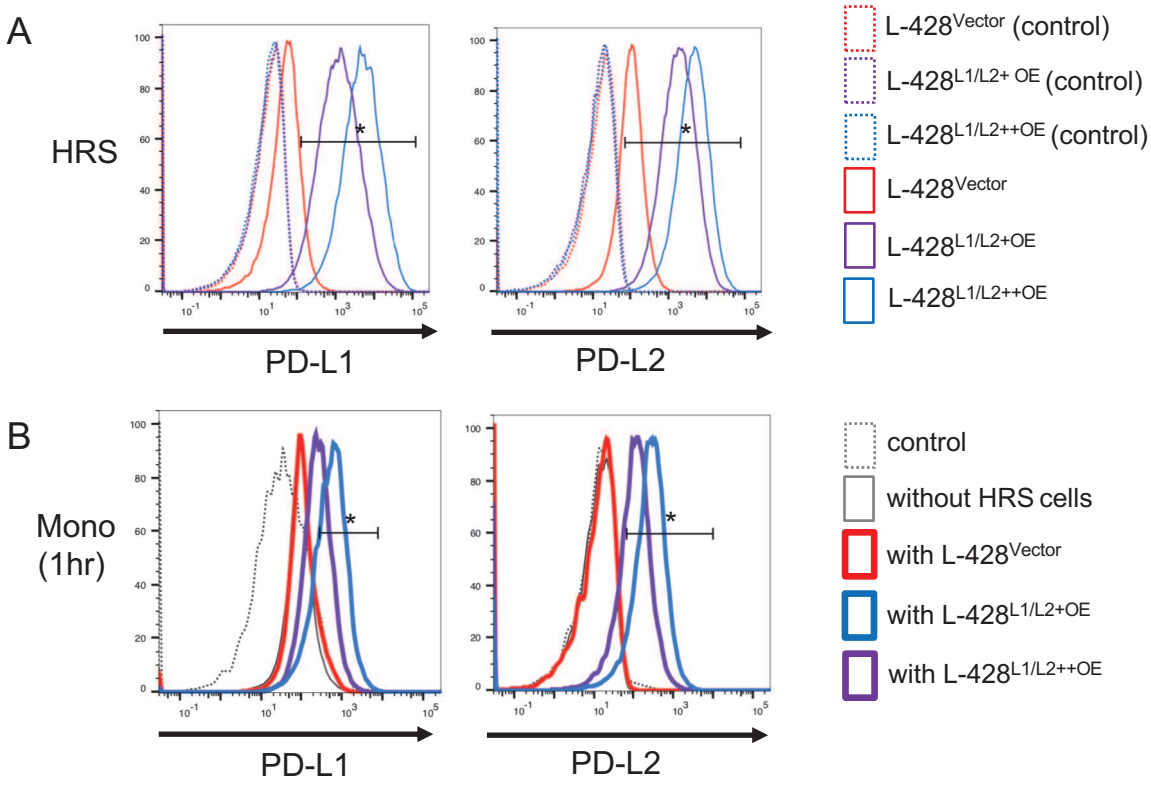

Supplemental Figure 6. The rate of trogocytosis-mediated PD-L1/L2 increase in monocytes were dependent on PD-L1/L2 expression levels of HRS cells. (A) Expression of PD-L1/L2 on two PD-L1/L2-overexpression cells (L-428$^{L1/L2+OE}$, L-428$^{L1/L2++OE}$) and control vector cells (L-428^{Vector}). MFI (PD-L1/PD-L2); L-428^{Vector} (control): 13.9/10.6, L-428$^{L1/L2+OE}$ (control): 13.2/7.52, L-428$^{L1/L2++OE}$ (control): 13.1/8.83, L-428^{Vector}: 62.1/128, L-428$^{L1/L2+OE}$: 2385/2889, L-428$^{L1/L2++OE}$: 8077/6399, *Positive cells (PD-L1/PD-L2); L-428^{Vector}: 10.5%/70.7%, L-428$^{L1/L2+OE}$: 96.2%/99.5%, L-428$^{L1/L2++OE}$: 99.4%/99.8%. (B) After monocytes were cultured with L-428$^{L1/L2+OE}$, L-428$^{L1/L2++OE}$ or L-428^{Vector} for one hour, expression of PD-L1/L2 on monocytes were analyzed by flow cytometry. MFI (PD-L1/PD-L2); control: 54.3/8.5, without HRS cells: 119/6.99, with L-428^{Vector}: 147/8.5, with L-428$^{L1/L2+OE}$: 349/154, with L-428$^{L1/L2++OE}$: 747/358. *Positive cells (PD-L1/PD-L2); without HRS cells: 6.17%/0.06%, with L-428^{Vector}: 11.2%/0.33%, with L-428$^{L1/L2+OE}$: 44.5%/71.1%, with L-428$^{L1/L2++OE}$: 75.3%/90.1%. The experiments were performed in triplicate, and representative histograms are presented.

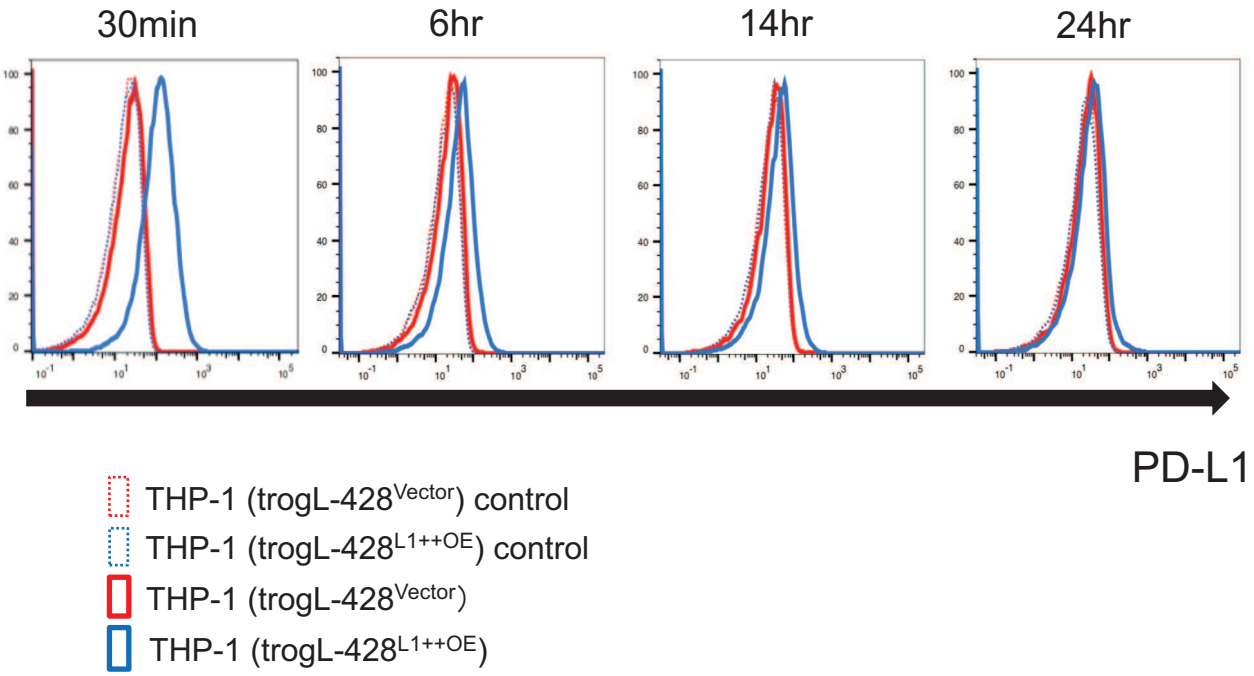

Supplemental Figure 7. Most of transferred PD-L1 on THP-1 (trogL-428^{L1++OE}) from HRS cells had disappeared at 6 hours.
THP-1 cells were co-cultured with L-428 control (L428^{Vector}) or L-428 PD-L1 overexpressing cells (L-428^{L1++OE}) for one hour, and then THP-1 cells were sorted, respectively (named as THP-1 (trogL-428^{Vector}) or THP-1 (trogL-428^{L1++OE})). PD-L1 on isolated THP-1 cells was examined by flow cytometry after 30 minutes, 6 hours, 14 hours, and 24 hours culture. The representative of two data were shown.

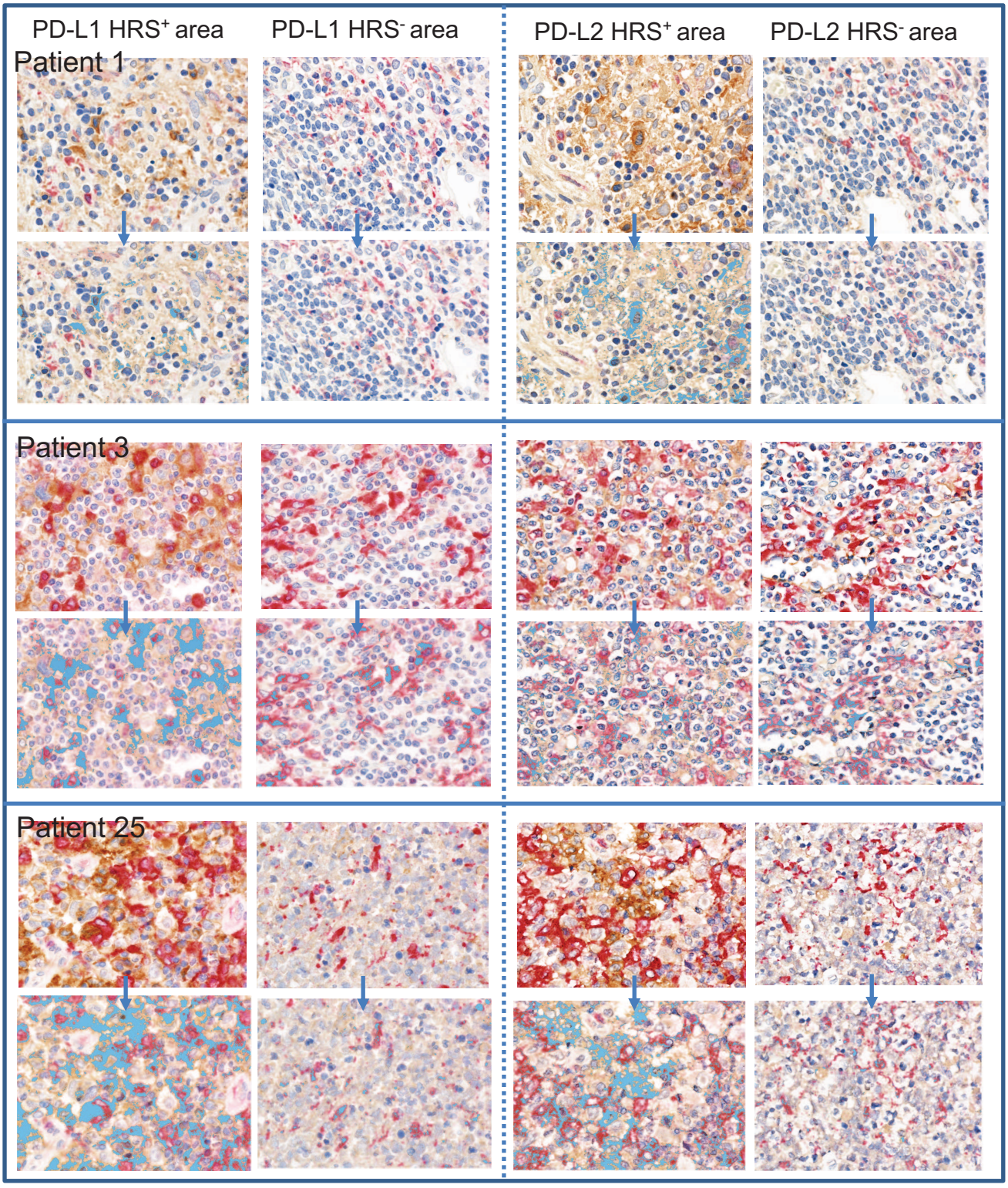

Brown: PD-L1 (left) or PD-L2 (right), Red: CD163, Blue: double immunostained area

Supplemental Figure 8. Representative data of PD-L1/L2 analysis in cHL human specimens.

Representative data of PD-L1 or PD-L2 and CD163 double immunostaining in each area (HRS^+ area and HRS^- area) are shown. PD-L1/L2 and CD163 double-positive area was visualized by icy (blue). Original magnification ×400.

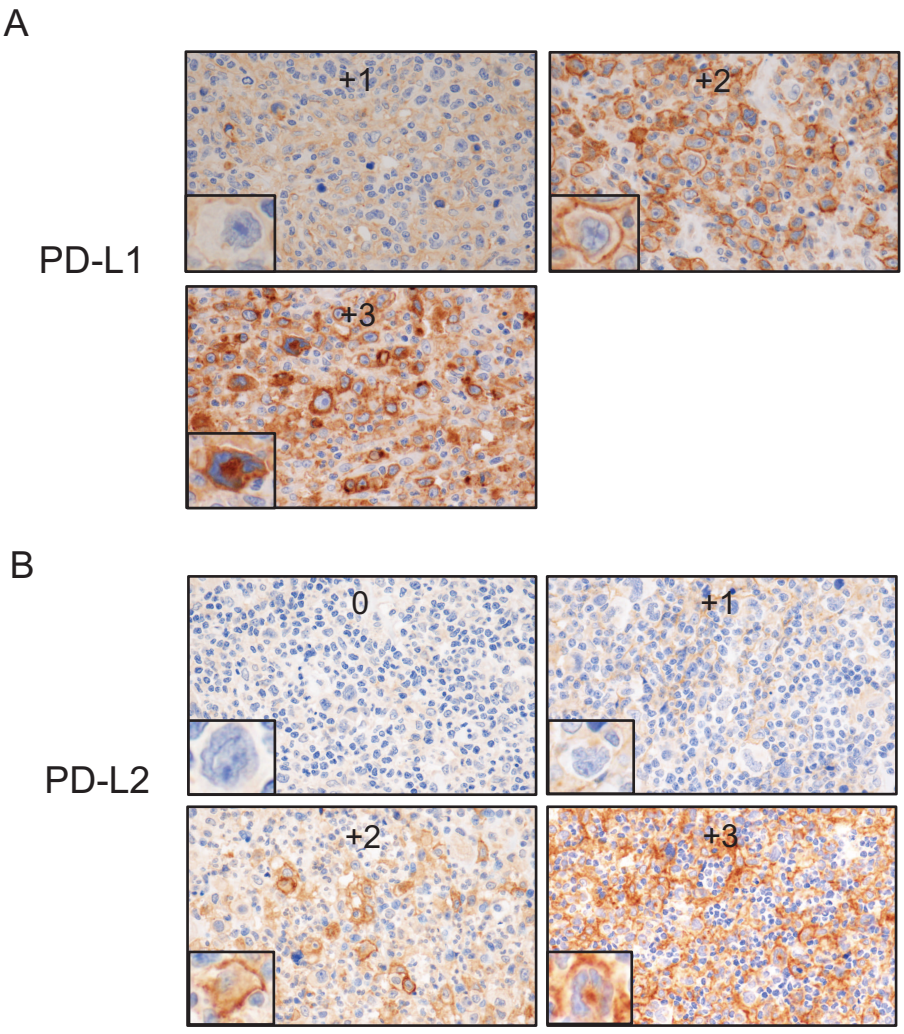

Supplemental Figure 9. The intensity of PD-L2 immunostaining was relatively weak compared to that of PD-L1 in cHL human specimens.
Representative figures of each intensity of PD-L1/L2 staining in cHL human specimens are shown. The PD-L1/L2 intensity of each cases referred to Supplemental Table 2. Original magnification ×400.

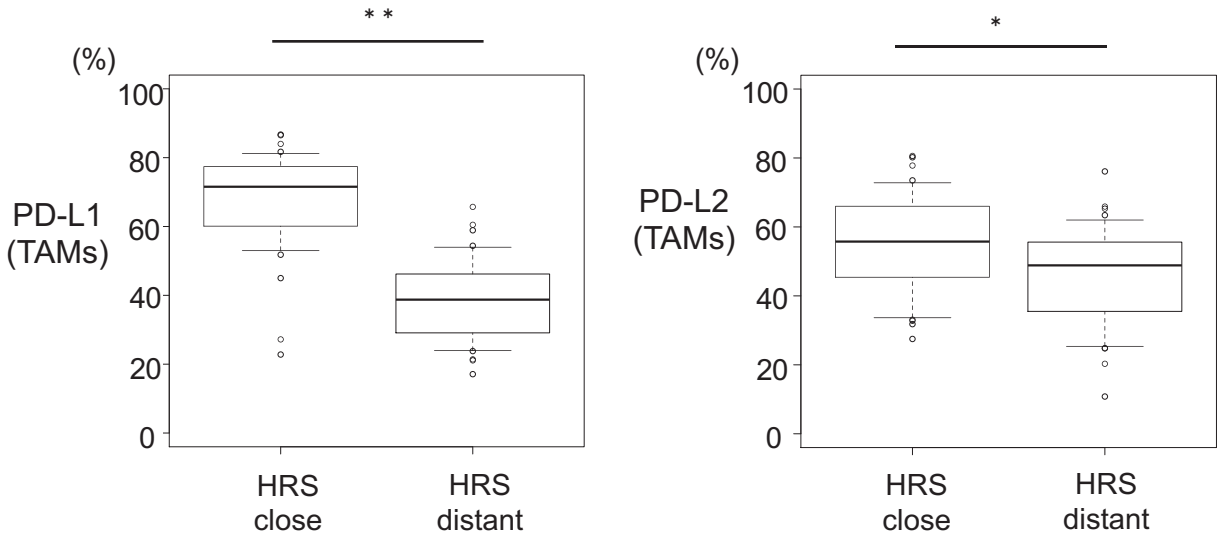

Supplemental Figure 10. Results of PD-L1/L2 expression on TAMs by ImageJ. PD-L1/L2 expression on TAMs between HRS-close and HRS-distant were measured and boxplots represent the data. The boxes denote the median, and the first and third quartile; the upper and lower whiskers represent the 90% and 10%, respectively (N = 38). The Wilcoxon signed-rank test was performed. *$P < 0.05$, ** $P < 0.001$.

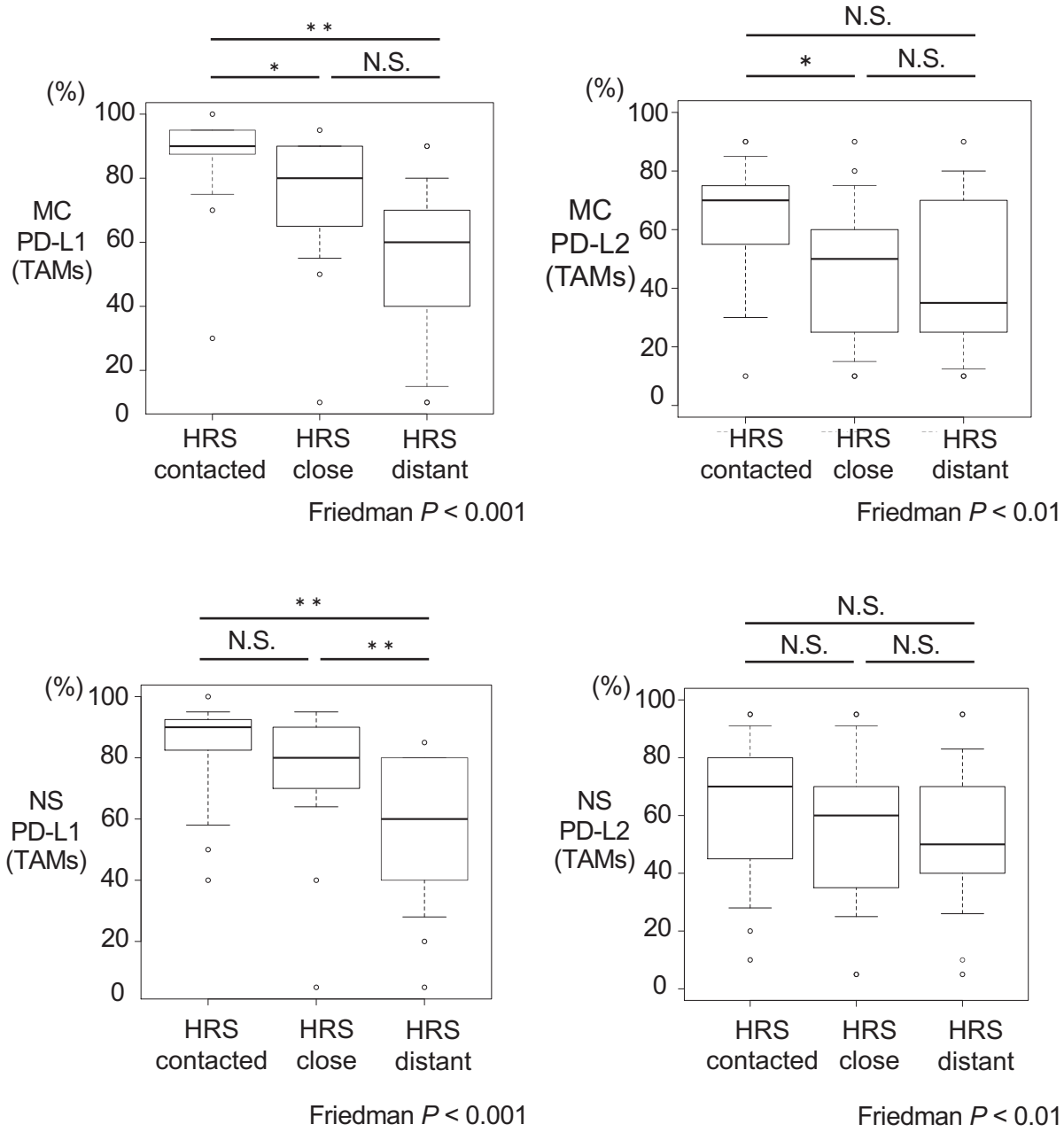

Supplemental Figure 11. Subtype analysis of cHL human specimens by pathologists' quantification.

PD-L1/L2 expression on TAMs among HRS-contacted, HRS-close and HRS-distant were measured and boxplots represent the data: mixed cellularity (MC, N = 16), nodular sclerosis (NS, N = 19). The boxes denote the median, and the first and third quartile; the upper and lower whiskers represent the 90% and 10%, respectively. The Friedman's test was performed, and Bonferroni correction was used for multiple comparisons. * $P < 0.05$, ** $P < 0.01$. N.S.: not significant.

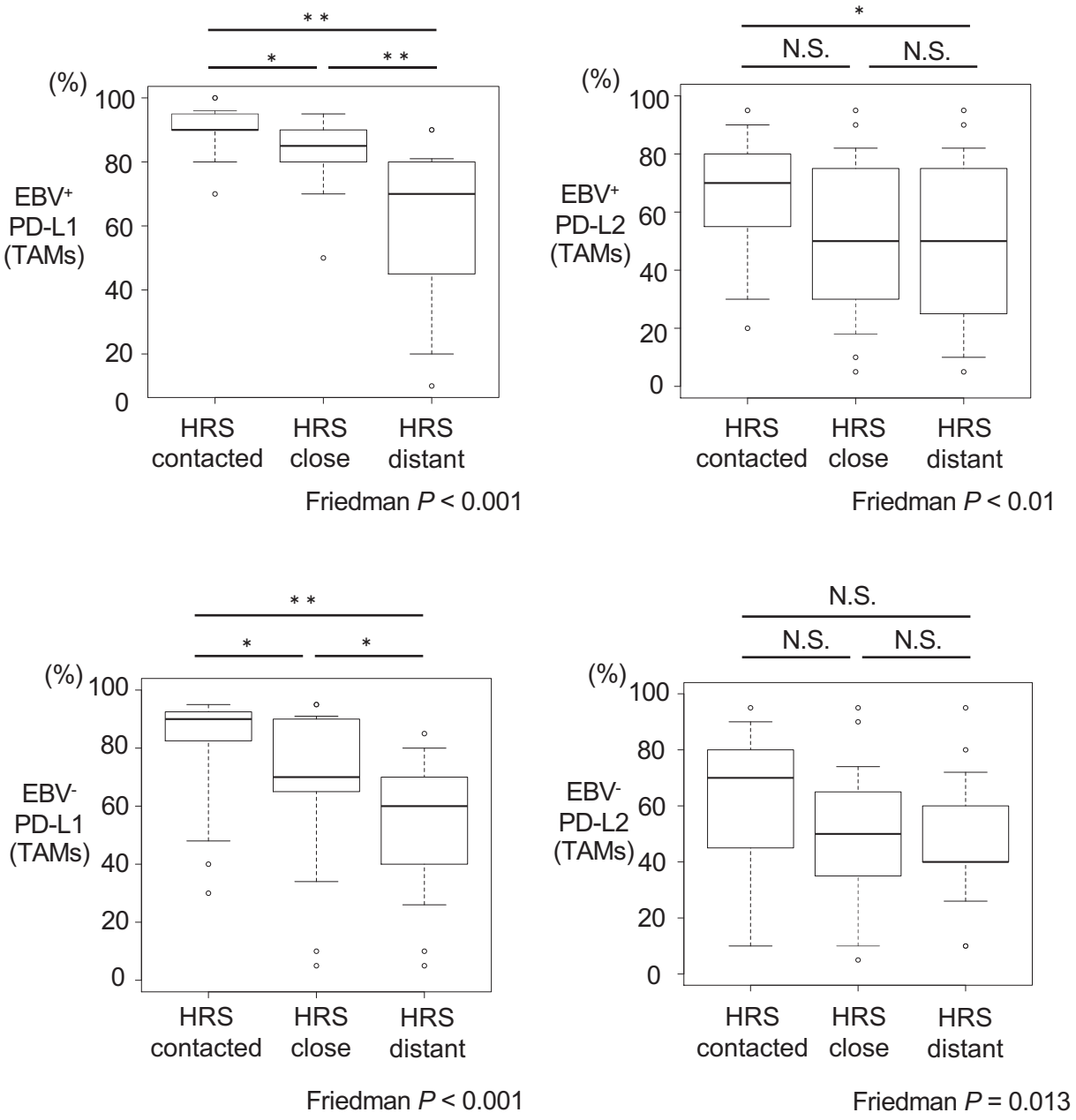

Supplemental Figure 12. Epstein-Barr virus positive or negative analysis of cHL human specimens by pathologists' quantification.

PD-L1/L2 expression on TAMs among HRS-contacted, HRS-close and HRS-distant were measured and boxplots represent the data: Epstein-Barr (EB) virus positive (EBV^+, N = 19), EB virus negative (EBV^-, N = 19). The boxes denote the median, and the first and third quartile; the upper and lower whiskers represent the 90% and 10%, respectively. The Friedman's test was performed, and Bonferroni correction was used for multiple comparisons. *$P < 0.05$, ** $P < 0.01$. N.S.: not significant.

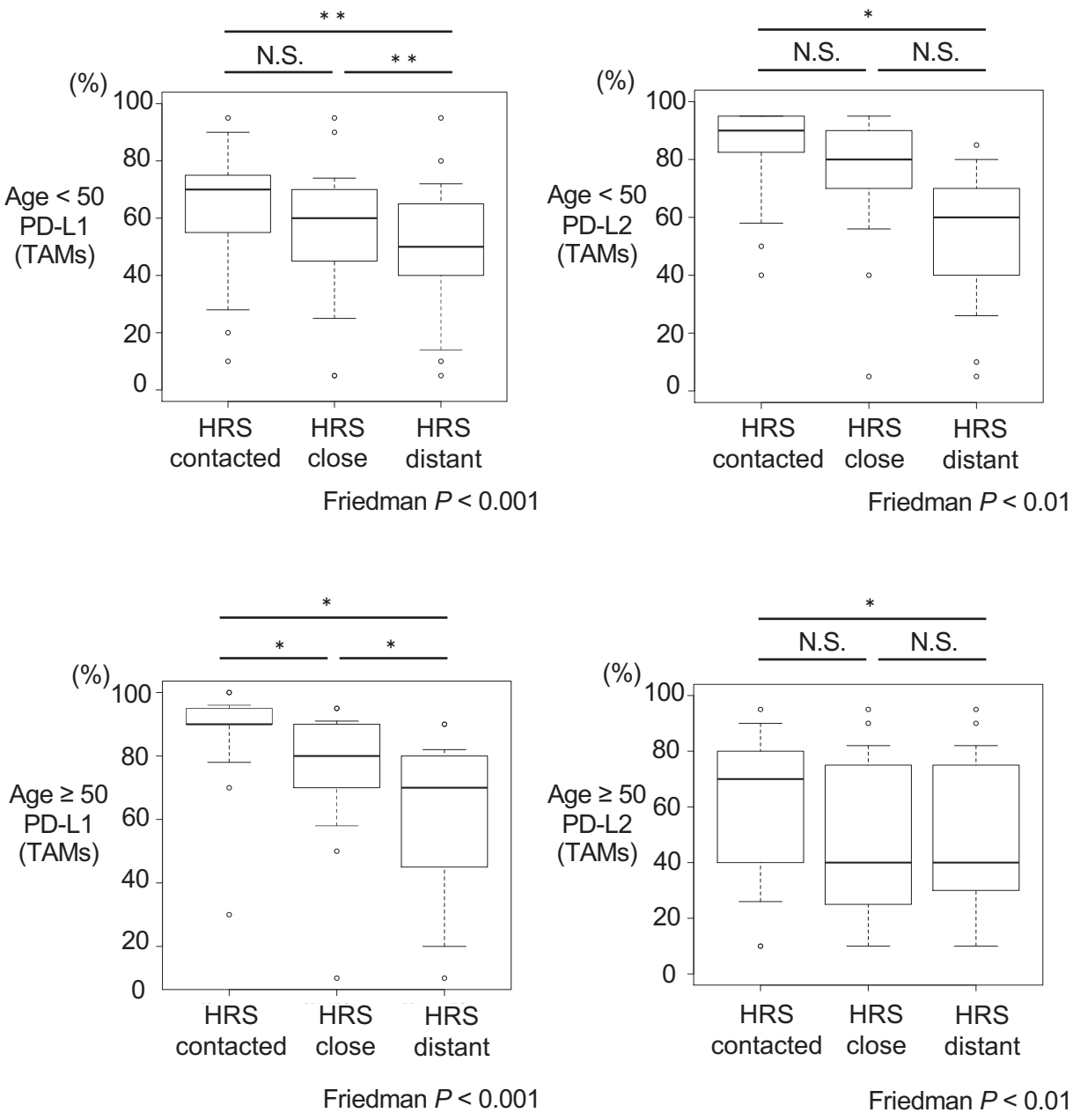

Supplemental Figure 13. Age < 50 or Age ≥ 50 analysis of cHL human specimens by pathologists' quantification.

PD-L1/L2 expression on TAMs among HRS-contacted, HRS-close and HRS-distant were measured and boxplots represent the data: Age < 50 (N = 19), Age ≥ 50 (N = 19). The boxes denote the median, and the first and third quartile; the upper and lower whiskers represent the 90% and 10%, respectively. The Friedman's test was performed, and Bonferroni correction was used for multiple comparisons. *P < 0.05, ** P < 0.01. N.S.: not significant.

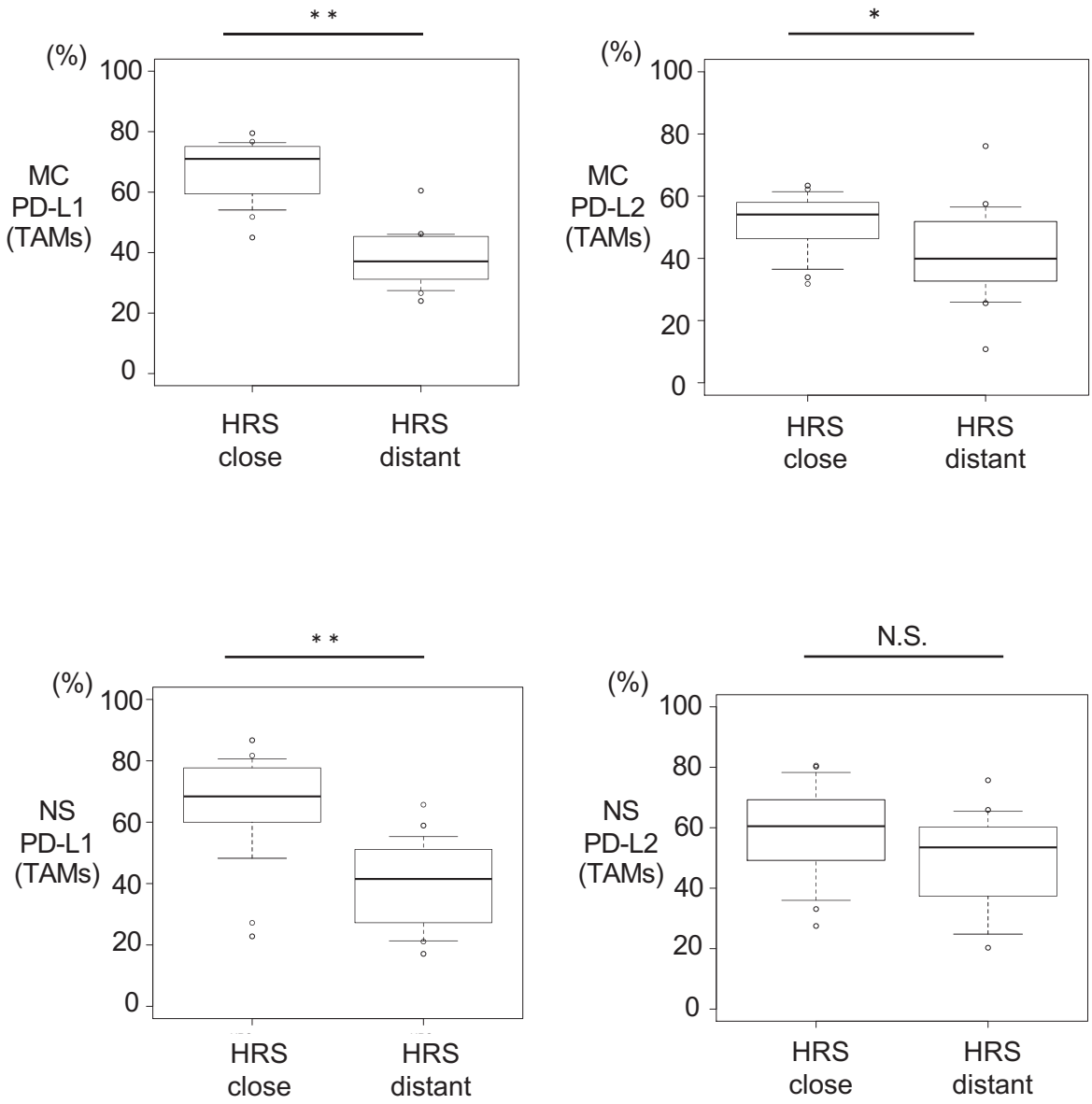

Supplemental Figure 14. Subtype analysis of cHL human specimens by ImageJ. PD-L1/L2 expression on TAMs between HRS-close and HRS-distant were measured and boxplots represent the data: mixed cellularity (MC, N = 16), nodular sclerosis (NS, N = 19). The boxes denote the median, and the first and third quartile; the upper and lower whiskers represent the 90% and 10%, respectively. The Wilcoxon signed-rank test was performed. * $P < 0.05$, ** $P < 0.01$. N.S.: not significant.

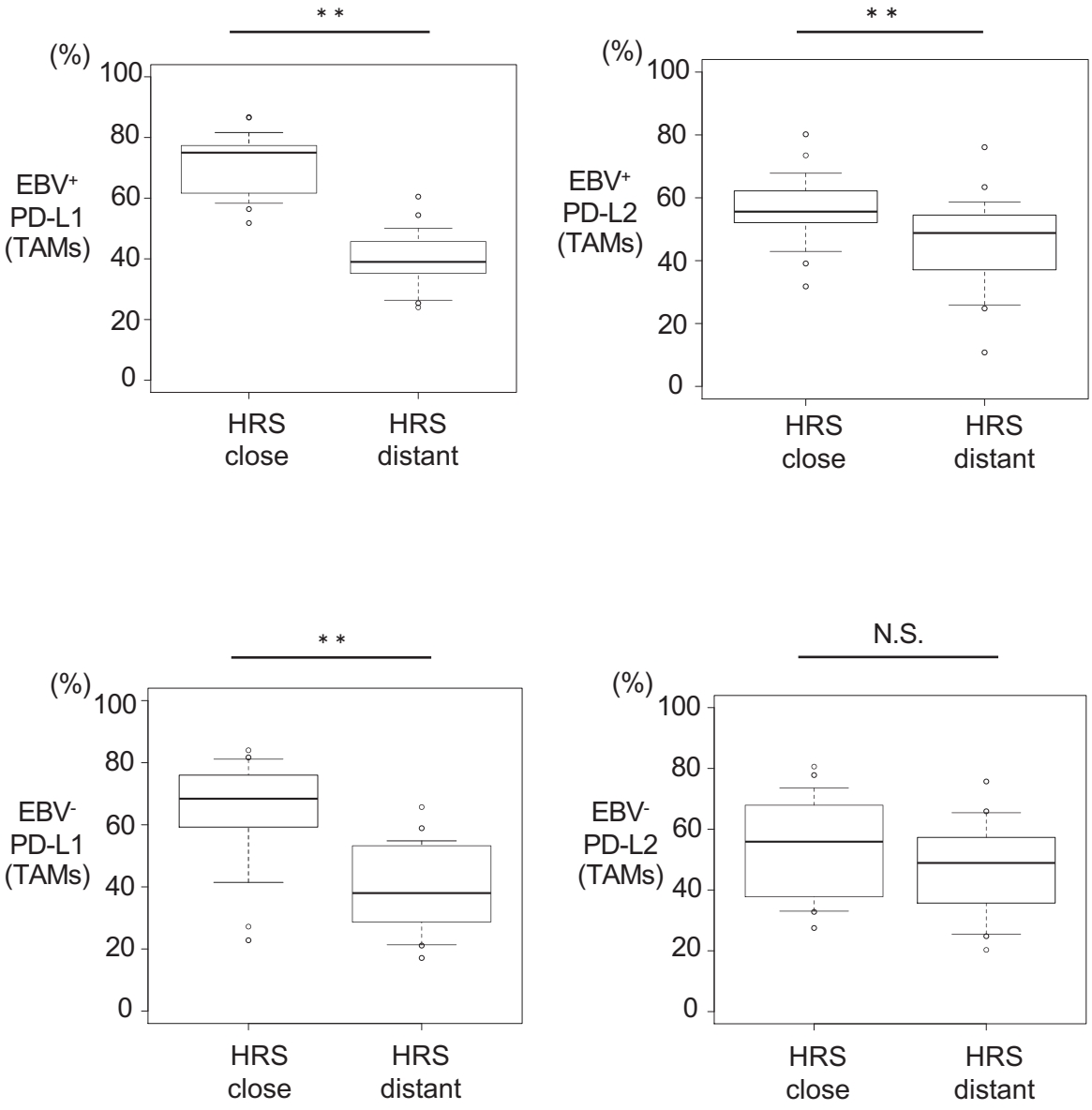

Supplemental Figure 15. Epstein-Barr virus positive or negative analysis of cHL human specimens by ImageJ.

PD-L1/L2 expression on TAMs between HRS-close and HRS-distant were measured and boxplots represent the data: Epstein-Barr (EB) virus positive (EBV^+, N = 19), EB virus negative (EBV^-, N = 19). The boxes denote the median, and the first and third quartile; the upper and lower whiskers represent the 90% and 10%, respectively. The Wilcoxon signed-rank test was performed. ** $P < 0.01$. N.S.: not significant.

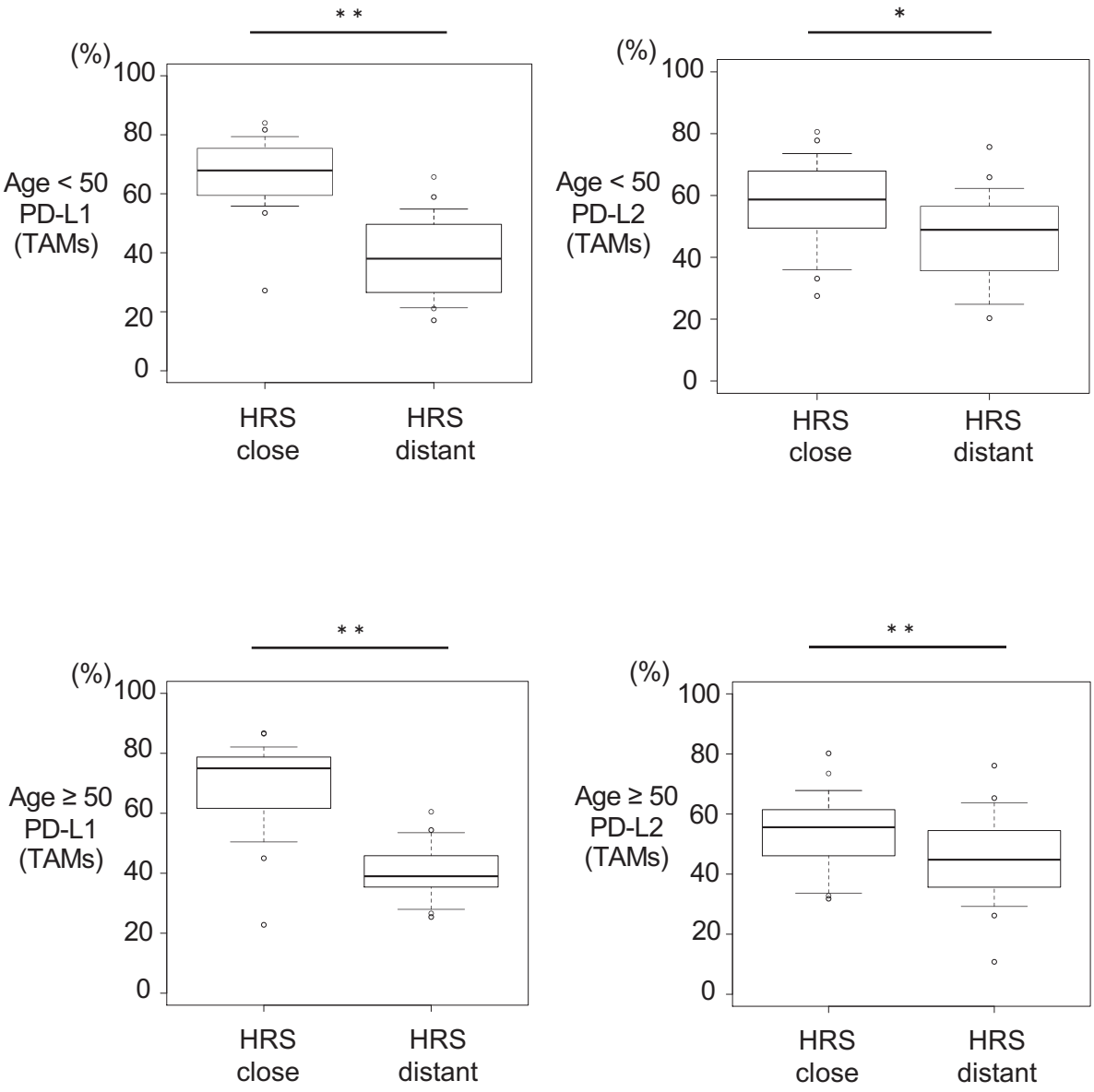

Supplemental Figure 16. Age < 50 or Age ≥ 50 analysis of cHL human specimens by ImageJ.

PD-L1/L2 expression on TAMs between HRS-close and HRS-distant were measured, and boxplots represent the data: Age < 50 (N = 19), Age ≥ 50 (N = 19). The boxes denote the median, and the first and third quartile; the upper and lower whiskers represent the 90% and 10%, respectively. The Wilcoxon signed-rank test was performed. *$P < 0.05$, ** $P < 0.01$.

Supplemental Table 1. Characteristics of patients in the current study

Patients	Disease subtype	EBV status	Age at Diagnosis	Sex	Biopsy site	Biopsy Status
1	NS	N	26	F	LN (supraclavicular)	Pimary
2	NS	N	18	M	LN (neck)	Primary
3	MC	P	18	M	LN (neck)	Primary
4	NS	N	20	M	Lung	Primary
5	MC	P	67	M	LN (supraclavicular)	Primary
6	NS	N	36	M	LN (supraclavicular)	Primary
7	MC	P	43	M	LN (axilla)	Primary
8	MC	P	76	M	Mediastinal	Primary
9	NS	N	41	F	LN (neck)	Primary
10	NS	N	59	F	LN (supraclavicular)	Primary
11	MC	P	72	M	LN (groin)	Primary
12	LR	N	53	F	LN (neck)	Primary
13	MC	P	71	M	LN (submandibular)	Primary
14	NS	N	26	M	LN (groin)	Primary
15	MC	P	62	M	LN (neck)	Primary
16	NS	P	78	M	LN (retroperitoneum)	Primary
17	NS	P	29	M	LN (neck)	Primary
18	NS	N	41	F	LN (supraclavicular)	Primary
19	MC	P	74	F	LN (submandibular)	Primary
20	MC	P	51	M	LN (axilla)	Primary
21	NS	N	29	M	LN (neck)	Primary
22	CHL-NOS	P	72	M	LN (supraclavicular)	Relapse
23	CHL-NOS	N	19	F	Mediastinal	Primary
24	MC	N	34	M	LN (neck)	Primary
25	NS	N	23	F	Mediastinal	Primary
26	MC	P	60	M	LN (neck)	Primary
27	NS	N	27	F	LN (neck)	Primary
28	NS	N	33	M	LN (neck)	Primary
29	MC	N	62	M	LN (neck)	Primary
30	MC	N	68	F	LN (supraclavicular)	Primary
31	MC	P	47	M	LN (neck)	Primary
32	NS	N	33	F	LN (axilla)	Primary
33	MC	P	84	M	LN (neck)	Primary
34	NS	N	18	M	LN (axilla)	Primary
35	NS	P	83	F	LN (neck)	Primary
36	NS	P	63	M	LN (neck)	Primary
37	NS	P	74	M	LN (axilla)	Primary
38	MC	P	77	M	LN (para-aorta)	Primary

EBV: Epstein-Barr virus, NS: nodular sclerosis, MC: mixed cellularity, LR: lymphocyte rich, CHL-NOS: classical Hodgkin lymphoma, not otherwise specified, P: positive, N: negative, M: male, F: female, LN: lymph node

Supplemental Table 2. Results of PD-L1/L2 expression on TAMs by pathologists

Patients	PD-L1 HRScells (intensity)	PD-L1$^+$ TAM HRS-contacted (%)	PD-L1$^+$ TAM HRS-close (%)	PD-L1$^+$ TAM HRS-distant (%)	PD-L2 HRScells (intensity)	PD-L2$^+$ TAM HRS-contacted (%)	PD-L2$^+$ TAM HRS-close (%)	PD-L2$^+$ TAM HRS-distant (%)
1	3	40	5	5	2	40	40	40
2	1	90	70	70	1	70	70	70
3	2	95	90	70	2	70	70	70
4	2	95	70	40	0	30	30	10
5	2	100	90	90	1	50	50	80
6	3	90	90	40	1	60	60	40
7	3	95	80	60	1	70	50	30
8	2	70	80	50	1	30	20	20
9	3	85	70	30	1	80	60	40
10	2	90	80	80	2	80	30	30
11	3	95	90	20	2	70	30	30
12	2	95	90	80	2	10	10	10
13	2	90	80	60	2	60	10	10
14	2	95	90	70	3	90	90	80
15	3	90	50	10	2	30	20	10
16	3	90	90	80	3	30	30	30
17	1	95	95	80	1	20	5	5
18	1	90	70	70	1	70	40	40
19	3	90	95	50	2	90	80	70
20	3	90	90	90	2	90	90	90
21	3	90	95	30	2	60	60	60
22	2	95	95	80	2	80	80	80
23	2	95	90	70	2	90	50	50
24	2	90	60	10	3	60	60	60
25	3	95	80	60	3	90	70	40
26	2	90	70	70	1	70	50	50
27	3	80	40	40	2	10	5	60
28	2	60	80	80	2	50	50	50
29	2	30	10	40	1	10	10	30
30	3	90	60	60	0	80	40	40
31	3	80	80	40	1	70	50	15
32	3	50	70	40	2	70	70	70
33	2	85	70	70	2	60	60	80
34	2	90	95	85	3	95	95	95
35	3	100	90	40	2	95	95	95
36	3	80	80	20	1	80	80	50
37	3	90	80	80	2	70	70	70
38	3	95	70	70	2	80	30	30

Expression levels on PD-L1/L2 : 0, 1, 2, 3

Supplemental Table 3. Results of PD-L1/L2 expression on TAMs by ImageJ

Patients	PDL-1$^+$ TAM HRS-close (%)	PD-L1$^+$ TAM HRS-distant (%)	PD-L2$^+$ TAM HRS-close (%)	PD-L2$^+$ TAM HRS-distant (%)
1	68.4	21.1	70.8	54.3
2	27.2	45.3	51.9	75.7
3	56.4	36.3	58.7	57.5
4	53.5	30.9	36.7	20.3
5	76.0	60.5	62.2	76.1
6	74.6	46.1	72.5	49.4
7	58.8	45.9	48.8	48.8
8	76.7	37.5	52.0	44.8
9	78.8	21.4	38.8	35.5
10	22.8	43.8	48.3	65.3
11	72.4	28.4	54.6	35.4
12	81.0	53.3	32.8	30.2
13	51.8	26.6	53.6	52.5
14	67.3	65.7	60.5	65.9
15	75.2	45.2	39.1	10.8
16	80.4	54.4	66.4	38.8
17	76.2	41.5	66.0	24.8
18	60.1	58.9	33.1	24.8
19	79.5	39.0	57.3	39.3
20	69.6	45.5	31.8	26.2
21	60.3	38.0	67.7	61.4
22	86.5	41.8	73.5	49.8
23	84.0	53.2	68.1	44.3
24	74.5	35,2	63.4	25.6
25	77.4	53.8	80.6	50.8
26	60.1	34.0	43.9	30
27	58.4	23.8	27.5	55.5
28	81.7	53.3	55.9	48.9
29	45.0	36.8	33.9	39.6
30	73.8	28.3	60.7	35.9
31	67.9	24.0	52.2	40.2
32	64.6	17.1	77.8	59.1
33	75.0	37.4	55.6	55.5
34	70.7	29.1	50.1	35.9
35	86.7	38.5	80.2	63.4
36	59.9	25.4	62.2	53.5
37	78.0	49.0	60.4	55.7
38	63.2	46.2	55.6	51.2

Supplemental Table 4. Results of observation of CD30 expressed TAMs direct contact with HRS cells

Patients	$CD30^+$ TAM HRS-contacted
1	+
2	+
3	−
4	−
5	−
6	+
7	+
8	−
9	+
10	−
11	+
12	+
13	+
14	+
15	−
16	+
17	+
18	+
19	+
20	−
21	−
22	−
23	+
24	−
25	+
26	−
27	−
28	+
29	−
30	+
31	+
32	−
33	+
34	+
35	+
36	−
37	+
38	+

Legends for videos

Supplemental Video 1. THP-1 and HRS cell lines were maintained contact under semi-solid medium. (A)(B) 2 × 10^5 THP-1-Venus$^+$ (green) cells and 2 × 10^5 HRS-mOrange$^+$ cells (red) lines were co-cultured on semi-solid culture. After incubation for one hour, they were observed under confocal microscopy for one hour. HRS-mOrange$^+$ cells were (A) L-591, (B) L-1236, respectively. Original magnification ×20 for each video. Three independent experiments were performed, and the representative videos are shown.

Supplemental Video 2. Monocytes and HRS cell lines were maintained contact under semi-solid medium. (A)(B) PKH67-labeled monocytes (green) and HRS-mOrange$^+$ cells (red) were co-cultured on semi-solid culture. HRS-mOrange$^+$ cells were (A) L-591, (B) L-1236, respectively. Original magnification ×20 for each video. Three independent experiments were performed, and the representative videos are shown.

Supplemental Methods

Lentivirus vector transfer into HRS cell lines and THP-1

mOrange and Venus were introduced into HRS cell lines and THP-1 cells, using lentivirus, respectively. HEK293T cell was used as packaging cells to produce lentiviral particles. X-tremeGENE9 (Roche), pCAG KGPIR for gag, pCAG 4RTR2 for Rev/tat, and pCMV-G viral packaging construct were added to HEK293T cells. The viral supernatant added to HRS cell lines and THP-1 cells cultured in a 24-well plate, and infected with the desired lentiviral vector for 99 minutes. FACS ARIA III was performed to obtain transduced cells.

Cell culture

L-591, L-1236, L-428, and THP-1 were cultured in RPMI1640 medium (Wako) supplemented with 10% fetal bovine serum (Hyclone), 1% penicillin and streptomycin (Wako), 1% non-essential amino acids (Wako), and 50 μM 2-mercaptoethanol (Gibco) in a 50 ml flask. Cells were passaged twice a week. Cell supernatant for HRS cells was harvested as follows. HRS cells were cultured on 2.5 × 10^5/ml at 37℃ for 24 hours. Then, the supernatant was collected after filtration through a Millex® GV-PVDF filter (0.22um).

Isolation of monocytes and $CD3^+$ T cells from peripheral blood mononuclear cells

Human peripheral blood mononuclear cells (PBMCs) from healthy volunteer donors were isolated by Ficoll-Hypaque (Lymphoprep™, AxisShield PoC AS, Oslo, Norway). They were stained biotinylated anti-human CD14 antibody (HCD14, BioLegend, San Diego, CA) and then labeled with anti-biotin magnetic MicroBeads. PBMCs were also treated with APC-conjugated anti-human CD3 antibody (HIT3a, BioLegend), and subsequently with magnetically labeled anti-APC MicroBeads (Milteny Biotec). The desired population was purified by positive selection (AutoMACS: program possel; Milteny Biotec).

Time-lapse observation of interaction between cells in semi-solid medium

The semi-solid culture system using methyl cellulose was established to assess movement of HRS cells and monocytes. Monocytes were labeled with PKH67 (SIGMA-ALDRICH, Saint Louis, MO) following the manufacturer's protocol. The culture medium contained 20% fetal bovine serum, 2 μM of 2-mercaptoethanol,

30% MEM-α, and 50% methyl cellulose, and PKH67-labeled monocytes (5 × 10^5) and HRS-mOrange$^+$ cells (2 × 10^5) were mixed in this medium. Then, 1 ml of cultures were plated on 35 mm glass bottom dishes. After incubation at 37℃ for 24 hours, they were observed under a confocal microscope (LSM700, Carl Zeiss) and time-lapse imaging was performed every three minutes for one hour in order to follow monocytes and HRS cells (Z axis: 25 μm). Three-dimensional images were analyzed by Imaris software (Bitplane).

Transwell migration assay

Migration assays were performed using a transwell chamber system in 24-well culture plate (Corning Inc., NY, USA). Migration from HRS cells to monocytes was explored using an 8 μm pore membrane. Briefly, HRS-mOrange$^+$ cells were seeded on the upper chamber (1 × 10^5 cells/well) in a final volume of 100 μl, and monocytes (2.5 × 10^5 cells/well) on the lower chamber in a final volume of 500 μl. After three hours of incubation, cells in the lower chamber were collected and the number of mOrange$^+$ cells were counted by flow cytometry. CCL19 (Peprotech) was used as the positive control.

Migration from monocytes to HRS cells was evaluated by 5 μm pore membrane. Briefly, isolated CD14$^+$ monocytes were seeded in the upper compartment (2 × 10^5 cells/well) in a final volume of 200 μl, and supernatant of HRS cells in the lower chamber in a final volume of 600 μl. After three hours of treatment, migrated monocytes were collected and then CD14$^+$ and PI$^-$ were counted as live monocytes by flow cytometry. CCL2 (PrimeGene, Shanghai) was used for the positive control.

Flow cytometry analysis

Monocytes were stained biotinylated anti-human CD14, and subsequently, APC/Cy7-conjugated Streptavidin (BioLegend). A total of 1 × 10^5 monocytes and/or 1 × 10^5 HRS-mOrange$^+$ cells were cultured in a 96-well plate. Cells were analyzed using FACS Verse (BD Biosciences). Dead cells were excluded by PI (propidium iodide, Sigma) staining. Data were analyzed using FlowJo software (Tree Star). The other antibodies used to detect the expression of cell surface markers are listed as below: APC-conjugated anti-human PD-L1 (29E.2A3, BioLegend), PE/Cy7-conjugated anti-human PD-L2 (MIH18, BioLegend), APC-conjugated anti-human CD30 (BY88, BioLegend).

Exosome isolation by ultracentrifugation

Purified exosomes from HRS cell lines were isolated by ultracentrifugation. L-591 and L-1236 were cultured in RPMI-1640 medium three days, and cell supernatants were harvested. Exosomes were collected from the supernatants using ultracentrifugation at 110000 X g for 70 minutes. Collected exosomes were labeled with PKH26. The amount of in exosomes were measured by nanophotometer (Implen, Munich, Germany). Isolated exosomes were observed by transmission electron microscope (JEM-1400, JEOL, Tokyo, Japan).

Establishment of PD-L1/L2 knockout in L-1236 by CRISPR/Cas9 system

Single guide RNAs (sgRNAs) were constructed into pX330-U6-Chimeric_BB-CBh-hSpCas9. The primers for the sgRNAs are listed as below.

PD-L1: 5'-CACCGAGCTACTATGCTGAACCTTC-3' (Forward).
5'-AAACGAAGGTTCAGCATAGTAGCTC-3' (Reverse).
PD-L2: 5'-CACCGTTGGCAGGAACGCTGACGTT-3' (Forward).
5'-AAACAACGTCAGCGTTCCTGCCAAC-3' (Reverse).

Using NEON electroporation system (Invitrogen), pX330-sgRNA and pcDNA3-EGFP (Addgene) were transfected into L-1236mOrange^{+} according to the manufacturer's instructions. The PD-L1/L2-positive fractions (L-1236^{Vector}) and PD-L1/L2-negative fractions (L-1236$^{L1/L2KO}$) were separated using FACS ARIA III.

Establishment of PD-L1/L2 overexpression in L-428

PD-L1/L2-cloned and control vectors were prepared. The primers for cloning PD-L1/L2 are listed as below.

PD-L1: 5'-GGCGCTAGCCATGAGGATATTTGCTGTCTTTATA-3' (Forward).
5'-ATTGCGGCCGCTTACGTCTCCTCCAAATGTGTATC-3' (Reverse).
PD-L2: 5'-GCCGCTAGCCATGATCTTCCTCCTGCTAATGTTG-3' (Forward).
5'-ATTGCGGCCGCTCAGATAGCACTGTTCACTTCCCT-3' (Reverse).

PD-L1/L2 were cloned into the multiple cloning site of CSII-CMV-MCS-IRES2-Venus vector using restriction enzymes, NotI and BamHI. These vectors were transduced into a lentiviral system. After transductions into L-428, Venus-positive and two PD-L1/L2-positive fractions were sorted using FACS ARIA III (L-428$^{L1/L2+OE}$ and L-428$^{L1/L2++OE}$). Venus^{+} control vectors were also separated (L-428^{Vector}).

Functional quantification of $CD3^+$ T cells by qPCR and ELISA

PKH26-labeled THP-1 cells were mixed with L-428^{Vector} or L-428^{L1++OE} for one hour, and the THP-1 cells were isolated (named as THP-1 (trogL-428^{Vector}) or THP-1 (trogL-428^{L1++OE})). Purified $CD3^+$ T cells were pre-stimulated with anti-CD3 antibody 1 μg/ml (OKT3, BioLegend) for 24 hours. Then, the isolated THP-1 cells were co-cultured with post-stimulated $CD3^+$ T cells in a 96-well plate. After co-culture for two hours, the expression levels of $CD3^+$ T cells activation markers (CD69, IL-2, and IFN-γ) were evaluated by qPCR, and IFN-γ secretion was estimated by ELISA to assess the inhibitory effect of isolated THP-1 cells.

qPCR analysis

The cells were purified using Sepasol-RNA I Super G. RT- PCR was conducted with the High-Capacity Reverse Transcription Kit (Applied Biosystems), and quantification by real-time PCR was performed using the THUNDERBIRD SYBR qPCR Mix (TOYOBO CO., Life Science Department Osaka, Japan) following manufacturer's protocol. CD3 is used as $CD3^+$ T cell internal control. The amount of total RNA of $CD3^+$ T cell + isolated THP-1 was unified. The primers were as follows.

CD3: 5'-AAGATGGTTCGGTACTTCTGACTTGTG-3' (Forward).
5'-GTAGAGCTGGTCATTGGGCAACAGAGT-3' (Reverse).
CD69: 5'-CAAGTTCCTGTCCTGTGTGC-3' (Forward).
5'-GAGAATGTGTATTGGCCTGGA-3' (Reverse).
IL-2: 5'-AGAACTCAAACCTCTGGAGGAAG-3' (Forward).
5'-GCTGTCTCATCAGCATATTCACAC-3' (Reverse).
IFN-γ: 5'-TGACCAGAGCATCCAAAAGA-3' (Forward).
5'-CTCTTCGACCTCGAAACAGC-3' (Reverse).

ELISA

IFN-γ concentration in cell supernatants were measured by human IFN-γ ELISA Max™ Deluxe set (BioLegend) following the manufacture's protocol.

Immunohistochemistry and digital image quantification of PD-L1/L2 in TAMs in cHL.

The diagnosis of cHL conformed the criteria of the World Health Organization classification of 2016[1]. The evaluation and quantification of the several markers including both PD-L1 and PD-L2 marker followed the similar experimental procedures and strategies as previously described by Carreras J et. al[2, 3]. Immunohistochemistry (IHC) was performed using an automated equipment, the Leica Bond Max Automated IHC/ISH Stainer, following the manufacturer's instructions (Leica Microsystems K.K., Tokyo, Japan). In summary, the IHC procedure consisted of deparaffinization, hydration, peroxide block, post primary, polymer reagent, DAB chromogen and hematoxylin counterstain. For single staining, the Bond Polymer Refine Detection ready-to-use system was used (DAB chromogen, #DS9800, Leica), and for double immunohistochemistry the Bond Polymer Refine Red Detection was used for the second marker (Fast Red chromogen, kit based on alkaline phosphatase-linked polymer, #DS9390, Leica). First, the IHC for CD30, PD-L1, PD-L2 and CD163 were performed as single stainings. Secondly, PD-L1 (brown)/CD163 (red) and PD-L2 (brown)/CD163 (red) were performed as double IHC stainings. All IHC was performed in consecutive sections. The primary antibodies were against human CD30 (Internal domain, clone JCM182, #NCL-L-CD30-591, Novocastra/Leica), PD-L1 (Extracellular domain specific, rabbit mAb, clone E1J2J, #15165, Cell Signaling), PD-L2 (rabbit mAb, clone D7U8C, #82723, Cell Signaling) and CD163 (mouse mAb, clone 10D6, #NCL-L-CD163, Novocastra). BOND Epitope Retrieval Solution 2 was used for antigen retrieval (#AR9640, Leica). Of note, for PD-L1 and PD-L2 needed a more stringent procedure with retrieval on pressure cooker in microwave and signal enhancer. The histological features of the biopsies of the case of cHL were first evaluated on the Hematoxylin-Eosin staining and the locations of the clusters of CD30-positive Hodgkin and Reed-Sternberg (HRS) cells were identified under optical evaluation, using an Olympus BX63 automated research microscope. The representative areas of the several marker (i.e. CD30, CD163, PD-L1 and PD-L2) containing the HRS cells were subsequently stored using a digital microscope camera for further evaluation (DP73 camera and cellSens software; Olympus, Tokyo, Japan; Flexscan EV2785, EIZO Corporation, Ishikawa, Japan).

The expression of PD-L1 and PD-L2 by the CD163-positive tumor-associated macrophage in relationship to their distance to the HRS cells was performed using the double IHC stainings: First, the region of interest (ROI) were identified, digitalized and stored. Secondly, the images of the ROIs were

visualized on the Icy open-source image processing software for bioimaging (BioImage Analysis unit Institute Pasteur, version 1.9.10.0)[4]. The Color Picker Threshold application (version 1.2.0.2) was used to highlight the PD-L1 and PD-L2 marker on the double CD163/PD-L IHC slides. The color threshold for PD-L1 and PD-L2-positive was set up on the characteristic HRS cells, which served as internal control, and subsequently all the cases were analyzed consecutively to avoid bias with a focus on the PD-L1/L2 expression on the macrophages. With this procedure, always under the supervision of the pathologist, the percentage of PD-1 ligand expression on the TAMs area was recorded.

The intensity of PD-L1/L2 staining was evaluated on the single IHC slide as an ordinal variable while the percentage of macrophage area stained with PD-L1/L2 marker was assessed on the double IHC slides as a quantitative variable. The PD-L1/L2 IHC expression in macrophages was assessed in three different regions: (1) HRS-contacted: the distance from macrophages to CD30-positive HRS cells is within 5 μm (and most of the macrophages are in direct physical contact with HRS cells); (2) HRS-close: the macrophages to CD30-positive HRS cells is within 110 μm [(within an area delimited by a 400× microscopic magnification that contains $CD30^+$ HRS cells (HRS^+ area)]; and (3) HRS-distant: the macrophages that are not close to HRS cells [i.e. present in an area of ×400 magnification that does not contain $CD30^+$ HRS cells (HRS^- area)]. Each area is 130 μm × 170 μm. The consensus of two pathologists was considered as a final decision.

Besides the quantification using Icy software, a second quantification, based on the same ROIs, was performed using ImageJ software to identify the PD-L1/L2 expression on macrophages. The software quantification was performed in both the PD-L1/L2 HRS-positive area and HRS-negative area. The following formula was used for calculating each area: [CD163 and PD-L double-positive / CD163 single-positive + CD163 and PD-L double positive] × 100 (%). Of note, both the quantification strategy using Icy and ImageJ are comparable as they both used the same ROIs that were selected by the pathologist. ImageJ allows numbers with more decimals and it is more systematic. On the other hand, Icy strategy allows better correction of background.

Reference

1. Swerdlow SH, Campo E, Harris N, Jaffe ES, Pileri SA, Stein H, *et al.* WHO Classification of Tumours of Haematopoietic and Lymphoid Tissues (Revised 4th edition). 2017: Lyon: IARC;.

2. Carreras J, Lopez-Guillermo A, Fox BC, Colomo L, Martinez A, Roncador G, *et al.* High numbers of tumor-infiltrating FOXP3-positive regulatory T cells are associated with improved overall survival in follicular lymphoma. *Blood* 2006 Nov 1; **108**(9): 2957-2964.

3. Carreras J, Yukie Kikuti Y, Miyaoka M, Hiraiwa S, Tomita S, Ikoma H, *et al.* Genomic Profile and Pathologic Features of Diffuse Large B-Cell Lymphoma Subtype of Methotrexate-associated Lymphoproliferative Disorder in Rheumatoid Arthritis Patients. *The American journal of surgical pathology* 2018 Jul; **42**(7): 936-950.

4. de Chaumont F, Dallongeville S, Chenouard N, Herve N, Pop S, Provoost T, *et al.* Icy: an open bioimage informatics platform for extended reproducible research. *Nature methods* 2012 Jun 28; **9**(7): 690-696.